A previously overlooked, highly diverse early Pleistocene elasmobranch assemblage from southern Taiwan

Chia-Yen Lin Equal first author, [1], **Chien-Hsiang Lin** Corresp., Equal first author, [1], **Kenshu Shimada** [2, 3]

[1] Biodiversity Research Center, Academia Sinica, Taipei, Taiwan

[2] Department of Environmental Science and Studies and Department of Biological Sciences, DePaul University, Chicago, Illinois, The United States of America

[3] Sternberg Museum of Natural History, Fort Hays State University, Hays, Kansas, The United States of America

Corresponding Author: Chien-Hsiang Lin
Email address: chlin.otolith@gmail.com

The Niubu fossil locality in Chiayi County, southern Taiwan is best known for its rich early Pleistocene marine fossils that provide insights into the poorly understood past diversity in the area. The elasmobranch teeth at this locality have been collected for decades by the locals, but not formally described and have received little attention. Here, we described three museum collections of elasmobranch teeth (n = 697) from the Liuchungchi Formation (1.90–1.35 Ma) sampled at Niubu locality, with an aim at picturing a more comprehensive view of the past fish fauna in the subtropical West Pacific. The assemblage is composed of 23 taxa belonging to 10 families and is dominated by *Carcharhinus* and *Carcharodon*. The occurrence of †*Hemipristis serra* is of particular importance because it is the first confirmed Pleistocene record in the whole Northwest Pacific. We highlight the maximum body size of *Carcharodon carcharias* to be exceeding 4.8 m, along with the diverse fossil elasmobranchs, suggesting that a once rich and thriving marine ecosystem in an inshore to offshore shallow-water environment during the early Pleistocene in Taiwan.

A previously overlooked, highly diverse early Pleistocene elasmobranch assemblage from southern Taiwan

Chia-Yen Lin[1], Chien-Hsiang Lin[1,#], Kenshu Shimada[2,3]

[1] Biodiversity Research Center, Academia Sinica, Taipei, Taiwan
[2] Department of Environmental Science and Studies and Department of Biological Sciences, DePaul University, Chicago, Illinois, USA
[3] Sternberg Museum of Natural History, Fort Hays State University, Hays, Kansas, USA
[#] Equal contribution

Corresponding Author:
Chien-Hsiang Lin[1]
Biodiversity Research Center, Academia Sinica, Taipei, Taiwan
Email address: chlin.otolith@gmail.com

Abstract
The Niubu fossil locality in Chiayi County, southern Taiwan is best known for its rich early Pleistocene marine fossils that provide insights into the poorly understood past diversity in the area. The elasmobranch teeth at this locality have been collected for decades by the locals, but not formally described and have received little attention. Here, we described three museum collections of elasmobranch teeth (n = 697) from the Liuchungchi Formation (1.90–1.35 Ma) sampled at Niubu locality, with an aim at picturing a more comprehensive view of the past fish fauna in the subtropical West Pacific. The assemblage is composed of 23 taxa belonging to 10 families and is dominated by *Carcharhinus* and *Carcharodon*. The occurrence of †*Hemipristis serra* is of particular importance because it is the first confirmed Pleistocene record in the whole Northwest Pacific. We highlight the maximum body size of *Carcharodon carcharias* to be exceeding 4.8 m, along with the diverse fossil elasmobranchs, suggesting that a once rich and thriving marine ecosystem in an inshore to offshore shallow-water environment during the early Pleistocene in Taiwan.

Introduction
The Indo-West Pacific is regarded as one of the crucial marine biodiversity hotspots in the world. Most of the species are concentrated in the coral triangle area that has its northern limit extending to southern Taiwan. A remarkable 181 chondrichthyan species have been recorded in the modern fish fauna of Taiwan (Ebert et al., 2013), approximating over 15% of the total

number of global chondrichthyan species (Weigmann, 2016). Such species diversity is regarded as one of the highest biodiversity hotspots for elasmobranchs when considering the size of Taiwan (Ebert et al., 2013). However, how this remarkable chondrichthyan fauna was formed and evolved in the past are not well understood, primarily because relevant fossil records are traditionally overlooked or unstudied, despite being well-represented in the marine deposits of Taiwan. Thus, comparisons for associated fossil fauna and past biogeographic distribution are limited, particularly in the tropical-subtropical Pacific. Lin et al. (2021) highlighted the need for paleontological data for understanding the historical context of fish fauna and further recommended research potentials in the region.

In the Western Foothills of Taiwan, numerous Neogene to Quaternary strata are known to be rich in marine fossils (e.g., Ribas-Deulofeu, Wang & Lin, 2021; Lin & Chien, 2022; Lin et al., 2022). Among which, the early Pleistocene Liuchungchi Formation in Niubu area, Chiayi County, southwestern Taiwan is of particular research interest due to its abundance and diversity of marine fauna. The fauna includes mollusks (Hu, 1989; Xue, 2004), crabs (Hu, 1989; Hu & Tao, 2004; Xue, 2004), sea urchins (Hu, 1989; Xue, 2004), whale barnacles (Buckeridge, Chan & Lee, 2018), teleost skeletons (Tao, 1993) and otoliths (Lin et al., 2018), and elasmobranch teeth (Xue, 2004). Fossils from this area have been collected by the late W.-J. Xue during the 80's-00's, and currently this large and diverse collection (over 3,000 specimens) is mainly deposited in the Chiayi Municipal Museum, Chiayi City, Taiwan (CMM). There is a considerable number of elasmobranch teeth from Xue's collection that was partly reported by Xue (2004) in a form of photographic atlas without descriptions. Another collection donated by Prof. Hsi-Jen Tao (National Taiwan University) to the Biodiversity Research Museum, Academia Sinica, Taipei, Taiwan (BRMAS, http://museum.biodiv.tw/eng) is available. Additional small collection is also deposited in the National Taiwan Museum (NTM). The purpose of this present study is to properly document the occurrences of these elasmobranch fossils from the Liuchungchi Formation at the Niubu locality based on these two collections and few newly collected specimens. The diverse association of teeth provides opportunities for obtaining a more complete view of the Pleistocene elasmobranch fauna in the rarely explored subtropical West Pacific.

Geologic setting

Since the late Miocene, the Taiwan Island was gradually upheaved by the Penglai orogeny—the collision between the Chinese continental margin and the Luzon Arc—and, subsequently, a series of subsiding foreland basins were formed in the western Taiwan (Ho, 1976; Suppe, 1984; Lundberg et al., 1997; Lin & Watts, 2002; Nagel et al., 2013; Chen, 2016). These foreland basins gradually developed from north to south accumulating clastic sediments (Ho, 1967; Covey, 1984; Teng, 1990), and in the south, the basins have high deposition rates (700–900 m/Ma) due to deeper depositional environment (Chen, Huang & Yang, 2011). Thus, the depositional sequences reflect sea-level changes during the Quaternary that followed the 100 ky orbit eccentricity cycles (Chen, Huang & Yang, 2011; Chen, 2016). Meanwhile, thick pre-orogenic and synorogenic sediments infilling the foreland basin were squeezed and uplifted, which formed the 7–9 km Miocene to Pleistocene strata in the Western Foothills (Yu & Chou, 2001; Nagel et al., 2013).

The Liuchungchi Formation in Niubu area, Chiayi County is exposed along the Bazhang River (Fig. 1B). Four successive formations from east to west, lower to upper can also be observed along this river: the Liuchungchi Formation, Kanhsialiao Formation, Erhchungchi Formation, and Liushuang Formation (Stach, 1957; Chou, 1975; Chen, Huang & Yang, 2011; Chen, 2016; Fig. 1B, C). The age of the Liuchungchi Formation is 1.90–1.35 Ma (Chen, 2016), with a deposition rate of about 700 m/Ma in the lower section and 1,100 m/Ma upsection (Chen, Huang & Yang, 2011). The Liuchungchi Formation is composed of dozens of depositional sequences, each representing a 41 ky climate cycle (Chen, Huang & Yang, 2011; Chen, 2016). The depositional environment can be divided into two distinct parts, with the lower sequence composed of thick sandstone with cross bedding, parallel bedding, and strong bioturbation reflecting shoreface to the offshore transition zone, and the upper sequence composed of interbeds of sandstone and shale and storm sandstone indicating the inner offshore (Chen, Huang & Yang, 2011; Chen, 2016).

Materials & Methods

The fossil site is located in Niubu area, Chiayi County, southwestern Taiwan, about 15 km east of Chiayi City (Fig. 1A). The layers containing fossils are exposed along the Bazhang River, just downstream of a dam near a high-voltage tower, where they are readily accessible during the winter and dry seasons when the water level is low (Fig. S1). Fossil mollusks are very abundant in several of the condensed layers, as well as fragments of crabs, sea urchins, and fish bones (Fig. 2A) On the other hand, fossil shark teeth are rare based on both surface collecting and bulk sampling conducted during our several field trips in 2018–2022. Bulk sediment samples of over 830 kg (Sites 1–3 in Fig. 2B) were sieved from the loosely cemented siltstone without any sedimentary structure, yielding a large number of otoliths (Lin et al., unpublished data), but only one shark tooth and two ray teeth.

The BRMAS, CMM, and NTM collections (see above) analyzed here were collected from the surface exposure of the Niubu locality without sediment sieving procedure; however, the exact stratigraphic horizons and detailed lithologic character within the Liuchungchi Formation for each specimen are not known.

Stacked images of teeth were taken and measurements of crown height (CH), mesial crown edge length (MCL), basal crown width, (BCW) were noted wherever necessary. Specimens from the BRMAS are registered under ASIZF, CMM under CMM F, and those in the NTM are under NTM I. Because the Pleistocene is relatively close to modern times, the morphology of elasmobranch teeth has not changed much from that time to the present. Therefore, identifications of these fossil teeth were conducted by comparing them with teeth of extant taxa.

Systematic Paleontology

A summary of taxa and their numeric abundance are listed in Table 1. The elasmobranch assemblage contains more than 697 teeth and are identified to 11 families and 24 taxa. The classification scheme follows that of Nelson, Grande & Wilson (2016), except for the family Galeocerdonidae, which we follow Fricke, Eschmeyer & Van der Laan (2021). General morphological terminology follows that of Compagno (1984, 2002), Purdy et al. (2001), Shimada (2002b), Purdy (2006), and Ebert et al. (2013). The synonymy list is limited to relevant records from Taiwan (Huang, 1965; Uyeno, 1978; Hu & Tao, 1993; Xue, 2004; Tao & Hu, 2008).

Class Chondrichthyes Huxley, 1880
Order Lamniformes Berg, 1958
Family Carchariidae Müller & Henle, 1838
Genus *Carcharias* Blainville, 1816
Carcharias taurus Rafinesque, 1810
(Fig. 3A, B)

1978 *Odontaspis* sp.; Uyeno, pl. 1, fig. 5.

Referred specimens: n = 2: ASIZF0100320, CMM F0204.
Description: CH = 12.92–16.83 mm; MCL = 12.18–15.54 mm; BCW = 7.07–7.84 mm. The teeth are characterized by a slender, dagger-like main cusp and a single pair of small lateral cusplets. The crown exhibits no serration. The lingual protuberance of the root is prominent.
Remarks: The teeth of *Carcharias taurus* are similar to those of *Odontaspis noronhai* and *O. ferox* by having a slender main cusp and lateral cusplet. However, the lateral cusplets of *Odontaspis* are more pronounced than those of *C. taurus*, including the fact that teeth of *O. ferox* typically exhibit multiple pairs of lateral cusplets.

Family Alopiidae Bonaparte, 1835
Genus *Alopias* Rafinesque, 1810
Alopias cf. *vulpinus* (Bonnaterre, 1788)
(Fig. 3C)

Referred specimen: n = 1: ASIZF0100532.
Description: CH = 3.23 mm; MCL = 4.39 mm; BCW = 3.78 mm. The tooth has a distally inclined, broadly triangular crown without serration. The apex of the cusp is slightly abraded.

The labial face of the crown is flat, whereas its lingual face is convex. The central foramen of the root is not clear on the lingual face. The base of the root is straight.

Remarks: The teeth of *Alopias vulpinus* are usually described as having a bilobated and arched root, with the crown extending or overhanging the root. However, these features are not seen in ASIZF0100532 presumably in part due to taphonomic abrasion.

Family Lamnidae Bonaparte, 1835

Genus *Carcharodon* Smith, 1838

Carcharodon carcharias (Linnaeus, 1758)

(Fig. 4)

1978 *Carcharhinus* sp.; Uyeno, pl. 1, fig. 4, pl. 2, fig. 7.

1978 *Carcharodon carcharias*; Uyeno, pl. 3, figs. 12, 13.

2004 Elasmobranchii indet.; Xue, pl. 1, figs. 1–6, pl. 2, figs. 1–7, pl. 3, figs. 1, 2–7, pl. 7 fig. 2.

Referred specimens: n = 55: ASIZF0100322–0100346, 0100435, 0100465, 0100530. CMM F0001–F0005, F0007–F0010, F0012–F0022, F0210, F0212, F2824, F2825, F2830, NTM I01122, I01123.

Description: CH = 9.23–41.03 mm; MCL = 11.01–45.68 mm; BCW = 12.69–37.09 mm. The upper teeth (Fig. 4A–G) are broad and triangular. The cutting edge of both mesial and distal sides are almost straight with coarse serrations. The labial face of the crown is flat and the lingual face is convex, where the crown is erect and symmetric to slightly distally inclined depending on tooth positions. The root is slightly arched, and the nutritive foramina and transverse groove are not prominent or absent. The lower teeth (Fig. 4H–L) have a more robust but narrower serrated crown and bilobate roots with a rounded lingual face compared to upper teeth.

Remarks: The genus *Carcharodon* is represented by three species: †*C. hastalis*, †*C. hubbelli*, and *C. carcharias*. Whereas *C. hastalis*, that was traditionally placed in the genus *Isurus* or †*Cosmopolitodus*, lived through the Miocene and early Pliocene, †*C. hubbelli* in the late Miocene and *C. carcharias* in the early Pliocene–Recent form a single lineage of chronospecies by developing serrations on their teeth (Ehret et al., 2012). The specimens described in this present paper exhibit well-developed serration consistent with teeth of *C. carcharias* (e.g., Hubbell, 1996), and not like the teeth of *C. hubbelli* with weak serrations (Erhet et al., 2012). They include the largest dental remains among all the shark tooth specimens described in this paper.

Genus *Isurus* Rafinesque, 1810

Isurus oxyrinchus Rafinesque, 1810

(Fig. 5)

?1965 *Isurus hastalis*; Huang, pl. 22, figs. 12–14.
1993 *Isurus hastalis*; Hu & Tao, pl. 24, figs. 6, 8.
2004 Elasmobranchii indet.; Xue, pl. 5, fig. 3, pl. 8, fig. 4.
2008 *Isurus* sp.; Tao & Hu, pl. 2, figs. 1–2.

Referred specimens: n = 6: ASIZF0100317–0100319, 0100321, CMM F0242, NTM I01131_1.
Description: CH = 9.86–27.81 mm; MCL = 12.21–26.89 mm; BCW = 9.96–9.31 mm. The mesial teeth have a slender, dagger-like, unserrated crown that is erect or lingually curved with an apical labial flexure (Fig. 5A–C). The root, if preserved, has two rather narrow lobes with a moderately tight basal concavity. The distal teeth have a flatter and broader, distally curved, unserrated crown with a short but mesiodistally wide root (Fig. 5D).
Remarks: Two extant species of *Isurus* are known: *I. oxyrinchus* and *I. paucus*. *Isurus oxyrinchus* has a more elongated and more labially curved crown than *I. paucus* (Whitenack & Gottfried, 2010). Teeth of *I. oxyrinchus* are also similar to those of *Carcharias taurus*, but teeth of *C. taurus* have a pair of lateral cusplets that is absent in teeth of *I. oxyrinchus* (Wilmers, Waldron & Bargmann, 2021). Huang (1965) reported a tooth of †*I. hastalis* (= *Carcharodon hastalis*; see above) from the Pleistocene Cholan Formation in Hsinchu, northern Taiwan; however, its species identification is questionable where the whereabouts of the specimens is unknown for verification.

Order Carcharhiniformes Compagno, 1973
Family Hemigaleidae Hasse, 1878
Genus *Hemipristis* Agassiz, 1835
Hemipristis elongata (Klunzinger, 1871)
(Fig. 6A)

Referred specimen: n = 1: CMM F0232.
Description: CH = 5.21 mm; MCL = 8.73 mm; BCW = 6.50 mm. This upper tooth possesses a triangular crown that is strongly directed distally. Both cutting edges are coarsely serrated except the apex of the crown that is smooth. The root is rectangular with a straight base, and its low lingual protuberance exhibits a prominent nutritive groove.
Remarks: See under †*Hemipristis serra* for morphological differences on the teeth of †*H. serra* and *H. elongata*. *Hemipristis elongata* is the only extant member of the genus, widely distributed in the continental and insular shelves of West Pacific and Indian Ocean (Ebert et al., 2013). The species has been very rare in the modern waters of Taiwan, but historical records (in 1988) indicate that it was once common in Keelung fish port, north Taiwan (Ebert et al., 2013).

†*Hemipristis serra* Agassiz, 1843
(Fig. 6B–D)

1978 *Hemipristis serra*; Uyeno, pl. 1, fig. 2.
2004 *Hemipristis* sp.; Xue, pl. 5, figs. 1, 2, 5, 6, 7.
2004 Elasmobranchii indet.; Xue, pl. 5, fig. 5, pl. 7, figs. 3, 5, pl. 9, figs. 6, 7.
2008 *Hemipristis serra*; Tao & Hu, pl. 6, fig. 1.

Referred specimens: n = 6: ASIZF0100460–0100462, CMM F2826, F2827, NTM I01131_2.
Description: CH = 18.98–25.86 mm; MCL = 21.72–36.68 mm; BCW = 20.25–30.23 mm. All collected specimens of this taxon represent upper right teeth that are characterized by a distally inclined, broad triangular crown, and mesiodistally spread bilobate root. Coarse serrations are present along the distal cutting edge, whereas serrations along the meisal cutting edge are finer than those along the distal side. The root has a prominent lingual protuberance with a deep nutritive groove, and has a notch-like shallow basal concavity. The boundary of the crown and root, especially on the lingual face, is strongly arched and protruding to the cusp.
Remarks: As presumed sister species, the teeth of extinct †*Hemipristis serra* and extant *H. elongata* are similar. However, compared to †*H. serra*, teeth of *H. elongata* possess a more gracile crown and a longer apex without serration, and a narrower root (Smith, 1957; Purdy et al., 2001). The Pleistocene records of †*H. serra* are rare globally compared to its Neogene records (Yabumoto & Uyeno, 1994; Carrillo-Briceño et al., 2015; Ebersole, Ebersole & Cicimurri, 2017; Boessenecker, Boessenecker & Geisler, 2018).

Family Carcharhinidae Jordan & Evermann, 1896
Genus *Carcharhinus* Blainville, 1816

Remarks: The identification based on teeth below the genus level is difficult for *Carcharhinus* (Compagno, 1984, 1988; Purdy et al., 2001; Naylor & Marcus, 1994; Marsili, 2006; Voigt & Weber, 2011; Ebert, Dando & Fowler, 2021). Most of the upper teeth are triangular with their crown inclined to the distal side. In different species, the crown varies from narrow to broad, and has smooth to coarsely serrated cutting edges, different notch angles on distal cutting edges, and the straight to convex mesial cutting edge. At least nine species of *Carcharhinus* are recorded in our material: *C. altimus*, *C. amboinensis*, *C. leucas*, *C. limbatus*, *C. longimanus*, *C. obscurus*, *C. plumbeus*, *C. sorrah*, and *C. tjutjot*. See remarks below for comparisons among other similar-looking species.

Carcharhinus altimus (Springer, 1950)
(Fig. 7)

Referred specimens: n = 17: ASIZF0100357, 0100359, 0100362, 0100363, 0100365, CMM F0080, F0101, F0113, F0134, F0214, F0224, F0293, F0304, F0322, F0363, TNM I01125, I01129_1.

Description: CH = 8.42–9.82 mm; MCL = 9.20–12.72 mm; BCW = 7.75–10.92 mm. The specimens of this species in this study consist only of upper teeth. The crown of the upper teeth is finely serrated and varies in shape from tall triangle to distally oblique. There is a notch on the distal cutting edge, whereas a slight constriction occurs on the lower part of the mesial cutting edge. The root is arched and has a nutritive groove. The roots of some specimens are not well-preserved (Fig. 7A, C, E, F), but where well-preserved (Fig. 7B, D), it is arched and exhibits a nutritive groove on the lingual face.

Remarks: Teeth of *Carcharhinus altimus* and *C. plumbeus* are similar. However, those of *C. altimus* exhibit a distally bent crown apex unlike those of *C. plumbeus* that show an apically directed crown apex (Figs. 7 vs. 13).

Carcharhinus amboinensis (Müller & Henle, 1839)
(Fig. 8)

Referred specimens: n = 7: ASIZF0100366, 0100368, 0100369, 0100419, 0100425, CMM F0209, F0229.

Description: CH = 6.88–13.79 mm; MCL = 9.28–20.48 mm; BCW = 9.16–21.74 mm. The triangular crown of the teeth is broad and exhibits coarse serrations although the serrations become smaller towards the crown apex. A prominent tooth neck is present between the crown and root on the lingual face. There is a notch on the distal cutting edge, whereas the mesial cutting edge is nearly straight. The bilobed root is gently arched and has a nutritive groove on the lingual face.

Remarks: Teeth of *Carcharhinus amboinensis*, *C. leucas*, and *C. longimanus* are very similar (Marsili, 2006; Voigt & Weber, 2011). However, the angle of the notch on the distal cutting edge of *C. longimanus* is larger than *C. leucas*, whereas the crown of *C. amboinensis* has a slightly wider base, more gracile apex, and stronger distal inclination than that of *C. leucas*.

Carcharhinus leucas (Valenciennes, 1839)
(Fig. 9)

?1965 *Carcharhinus gangeticus*; Huang, pl. 22, figs. 19, 20.
2004 Elasmobranchii indet.; Xue, pl. 3, fig. 2, pl. 4, fig. 3, pl. 7, fig. 7, pl. 9, fig. 4.

Referred specimens: n = 71: ASIZF0100390, 0100393–0100398, 0100400–0100404, 0100411, 0100481, 0100424, CMM F0154, F0155, F0157, F0159, F0162, F0163, F0165–F0168, F0170–F0175, F0180, F0183, F0186–F0188, F0190, F0192, F0198–F0201, F0205, F0206, F0221, F0222, F0227, F0231, F0240, F0244, F0246, F0249, F0288, F0290, F0297, F0299, F0301, F0317, F0319, F0321, F0328, F0332, F0334, F0341, F0342, F0348, F0354, F0362, NTM I01130_2.

Description: CH = 8.64–18.68 mm; MCL = 9.98–21.69 mm; BCW = 10.81–30.56 mm. The teeth of *C. leucas* are generally robust. The crown of the upper teeth (Fig. 9A–H) is broad and triangular with a slight distal inclination. The middle of the distal cutting edge is concave as its middle portion forms a weak notch, whereas the mesial cutting edge is straight to slightly convex. Both cutting edges are coarsely serrated, but the sizes of serrations are smaller at the base and apex of the crown than those in the middle. The boundary between the crown base and root on the lingual face displays a V-shape tooth neck. The bilobate root is arched and displays weak nutritive grooves on the lingual face (Fig. 9A–D, F). The lower teeth (Fig. 9I), that have fine serrations, are labiolingually thicker and mesiodistally narrower than the upper teeth.
Remarks: Marsili (2006) described that the crown of *Carcharhinus longimanus* is larger, elongate and the margin of the root is straight compared with that of *C. leucas*. In addition, based on the images of *Carcharhinus* by Voigt & Weber (2011), we find some other slight differences between the upper teeth of the two species: the angle on the distal cutting edge of *C. longimanus* is larger than that of *C. leucas*, making the crown of *C. leucas* inclines more distally than that in *C. longimanus*. The tooth shape of *C. leucas* is close to a wide-bottom triangle, whereas a taller triangle is seen in *C. longimanus*.

Carcharhinus limbatus (Valenciennes, 1839)
(Fig. 10)

1978 *Carcharhinus* sp.; Uyeno, pl. 3, fig. 14.
2004 Elasmobranchii indet.; Xue, pl. 8, fig. 5.

Referred specimens: n = 42: ASIZF0100467–0100480, 0100482, 0100483, CMM F0049, F0056, F0108, F0111, F0216, F0217, F0234, F0236–F0238, F0286, F0289, F0291, F0295, F0306, F0307, F0310, F0368, F0369–F0373, NTM I01127, I01133_2, I01134_2.
Description: CH = 7.70–9.31 mm; MCL = 10.02–13.26 mm; BCW = 10.26–14.70 mm. Our specimens of this species consist only of upper teeth. The teeth of *C. limbatus* are serrated and are characterized by a narrow cusp that is erect to slightly oblique distally, with a mesiodistally sprawled crown base. The serrations near the crown base are coarser than those towards the crown apex. The root is apicobasally shallow. Its base is straight to slightly arched with a prominent deep nutritive groove that forms a notch along the root base.
Remarks: Although similar, teeth of *Carcharhinus limbatus* can be distinguished from those of *C. brachyurus* and *C. brevipinna*. The serrations on the cutting edges in *C. brevipinna* are absent or weak, and in *C. brachyurus*, the apex is more pointed and more distally directed than in *C. limbatus*. In addition, the crowns of *C. limbatus* have a narrow, erect cusp with a sharp transition to their broad crown base that is distinct from all other congeneric specimens in our material.

Carcharhinus longimanus (Poey, 1861)
(Fig. 11)

1965 *Carcharhinus gangeticus*; Huang, pl. 22, figs. 21, 22.
2004 Elasmobranchii indet.; Xue, pl. 4, fig. 4, pl.7, fig. 6, pl. 9, fig. 1.

Referred specimens: n = 35: ASIZF0100370, 0100371, 0100373–0100382, 0100391, 0100392, 0100422, 0100428, 0100421, 0100466, CMM F0006, F0011, F0087, F0146, F0151, F0153, F0156, F0158, F0182, F0189, F0194, F0195, F0197, F0223, F0248, F0287, F0294, NTM I01128, NTM I01130.
Description: CH = 10.23–15.93 mm; MCL = 13.51–22.08 mm; BCW = 13.20–21.69 mm. The crown of the upper teeth (Fig. 11A–H) is board, triangular, and coarsely serrated. The distal cutting edge is weakly concave, whereas the mesial cutting edge is nearly straight. The crown base on the lingual side is deeply concave that is accompanied by a narrow tooth neck and a deep bilobate root basally with a shallow nutritive groove. The lower teeth (Fig. 11I, J) are thicker and narrower than the upper teeth, they also have fine serrations on the cutting edges. The boundary between the crown base and root on the lingual side is also deeply concave with a V-shape tooth neck.
Remarks: See remarks under *C. leucas*.

Carcharhinus obscurus (Lesueur, 1818)
(Fig. 12)

2004 Elasmobranchii indet.; Xue, pl. 4, fig. 7.

Referred specimens: n = 25: ASIZF0100372, 0100383–0100389, 0100428, CMM F0123, F0143, F0148, F0160, F0164, F0176, F0177–F0179, F0181, F0184, F0196, F0208, F0338, F0353, NTM I1132_3.
Description: CH = 6.84–15.14 mm; MCL = 10.12–21.61 mm; BCW = 9.85–20.96 mm. The specimens of this species in this study consist only of upper teeth. They are broad and triangular with coarse serrations, although the serrations tend to become finer apically. The mesial cutting edge is overall slightly convex with a marked distally directed crown apex. The distal cutting edge has a relatively deep notch, but the degree of the angle varies based on tooth positions within the dentition. The crown base on the lingual side is moderately concave and is accompanied by a prominent tooth neck and a relatively robust bilobed root basally that has a shallow nutritive groove.
Remarks: The crown of *Carcharhinus obscurus* is mesiodistally broad and typically exhibits course serrations along the middle section of both cutting edges (Fig. 12), a feature for separating all other congeneric specimens in the present study.

Carcharhinus plumbeus (Nardo, 1827)
(Fig. 13)

Referred specimens: n = 50, ASIZF0100405–0100410, 0100412, 0100429, CMM F0074–F0077, F0079, F0086, F0088, F0091, F0096, F0100, F0106, F0115, F0124, F0144, F0169, F0225, F0228, F0292, F0302, F0316, F0318, F0320, F0325–F0327, F0330, F0331, F0333, F0335, F0337, F0346, F0347, F0349, F0350, F0352, F0356, F0360, F0361, F0364, F0365, F0367, NTM I01124.

Description: CH = 6.28–12.17 mm; MCL = 7.81–17.06 mm; BCW = 7.48–13.39 mm. The teeth that are identified to this species in this study are all upper teeth. They are triangular with a slight distal inclination and with fine serrations. The mesial cutting edge is nearly straight, whereas the distal cutting edge tends to form a shallow notch close to the crown base. The root is bilaobate and arched, and a shallow nutritive groove is present on the lingual face.

Remarks: The crown of *Carcharhinus. plumbeus* is narrower and elongate than that of *C. leucas*, *C. longimanus*, *C. obscurus*, and *C. amboinensis*, but it is wider than that of *C. altimus*.

Carcharhinus sorrah (Valenciennes, 1839)
(Fig. 14)

Referred specimens: n = 11: ASIZF0100418, CMM F0117, F0119, F0122, F0126, F0129, F0135, F0140, F0303, F0343, F0344.

Description: CH = 4.39–5.80 mm; MCL = 5.55–9.82 mm; BCW = 4.03–9.85 mm. All teeth identified to this species in this study are all represented by upper teeth; their crown consists of a finely serrated triangular cusp that strongly inclines distally, that is distally followed by a coarsely serrated, relatively broad distal heel. The crown apex is narrow and may slightly recurved apically (Fig. 14C, D). The serrations on the distal heel become smaller distally, where finer secondary serrations are observed on one or two mesial-most serrations of the distal heel. Well-preserved specimens exhibit a strong nutritive groove on the lingual face that forms a notch along the root base.

Remarks: According to Voigt & Weber (2011), the crown of the upper teeth in *Carcharhinus sorrah* is high, and its distal cutting edge is deeply notched. These features are seen in our specimens, but their descriptions for the serrations and cusplets are slightly different. The serrations on the central part are coarser than those on the mesial cutting edges in Voigt & Weber (2011), whereas in our specimens, the coarsest serrations are on the basal part of the mesial cutting edges. Furthermore, the main cusp and distal cusplets in our specimens are farther apart than those figured by Voigt & Weber (2011). The teeth of *C. tjutjot* and *C. sorrah* are both characterized by a coarsely serrated distal heel, but the teeth of *C. tjutjot* differ from those of *C. sorrah* by having fewer but larger serrations forming a distal heel (Figs. 14 vs. 15).

Carcharhinus tjutjot (Bleeker, 1852)
(Fig. 15)

Referred specimens: n = 19: ASIZF0100413–0100417, CMM F0116, F0136–F0138, F0142, F0296, F0298, F0323, F0324, F0339, F0345, F0357, F0376, F0377.

Description: CH = 4.25–5.82 mm; MCL = 6.03–9.01 mm; BCW = 5.61–7.94 mm. The specimens of this species described here are all represented by upper teeth. They have a robust, distally inclined, triangular cusp, followed distally by a small distal heel consisting of coarse serrations that rapidly diminish in size distally. The strongly inclined mesial cutting edge is relatively straight, where the apex may slightly recurve apically and its serrations become slightly coarser towards the base. Finer secondary serrations are observed on the first and possibly second mesial-most serrations on the distal heel. The root is weakly bilobate as the root base is nearly straight. Well-preserved specimens show a shallow nutritive groove on the lingual face of the root.

Remarks: The teeth of *C. sealei*, *C. dussumieri*, *C. coatesi*, and *C. tjutjot* are very similar (White, 2012). The differences among them are the serrations on the cupslet and cutting edges. The serrations of *C. sealei* are present only on the basal half of the mesial cutting edge, where the distal cutting edge, including the distal heel are smooth (White, 2012). Both cutting edges of teeth in *C. coatesi* have fine to coarse serrations, but their distal heel is smooth. Both cutting edges of teeth, including the distal heel, in *C. dussumieri* have evenly-sized coarse serrations. The teeth of *C. tjutjot* also have evenly-sized serrated cutting edges, including the distal heel. *Carcharhinus dussumieri* and *C. tjutjot* have long been misidentified due to their similar appearance, but *C. dussumieri* is now considered a West Indian species distributed from the Persian Gulf to India, whereas *C. tjutjot* is distributed from Indonesia to Taiwan (White, 2012).

Genus *Negaprion* Whitley, 1940

Negaprion acutidens (Rüppell, 1837)

(Fig. 16A–C)

Referred specimens: n = 3: ASIZF0100531, 0100533, CMM F0203.

Description: CH = 7.20–13.83 mm; MCL = 7.03–13.7 mm; BCW = 5.51–6.82 mm. The teeth of this species in this study are all incomplete, missing the root lobes due to taphonomic abrasion, but they all preserve a slender, erect crown that has a highly convex lingual face. Both cutting edges are straight and without any serrations or crown base heels.

Remarks: The teeth of *Negaprion acutidens* and *Isurus oxyrinchus* are somewhat similar as their crowns are erect without serrations and lack lateral cusplets. However, the crown base of *N. acutidens* extends mesially and distally, whereas the crown base does not widely spread in *I. oxyrinchus*. *Negaprion acutidens* and *N. brevirostris* are two extant species of the genus, with *N. acutidens* distributed in Indo-West Pacific and the latter in the East Pacific and Atlantic (Ebert et al., 2013).

Genus *Rhizoprionodon* Whitley, 1929

Rhizoprionodon acutus (Rüppell, 1837)

(Fig. 16D–H)

Referred specimens: n = 8: ASIZF0100463, 0100464, CMM F0110, F0120, F0121, F0130, F0131, F0218.

Description: CH = 3.97–5.35 mm; MCL = 6.22–10.82 mm; BCW = 7.68–10.69 mm. The upper teeth of this species have a crown that is strongly inclined distally that is accompanied by a low distal heel (Fig. 16D–G). Both cutting edges, including the distal heel, are smooth or exhibit fine irregular serrations. The mesial cutting edge is overall straight, whereas the junction between the cusp and distal heel is deeply notched. A deep nutritive groove is present on the lingual side of the root that continues to the root base. The root is low with practically no basal concavity. ASIZF0100464 (Fig. 16H) is a lower tooth, where its crown that is unserrated is more gracil than the upper teeth with a concave mesial cutting edge that makes the crown apex to point apically. The root morphology is similar to that of lower teeth.

Remarks: The teeth of *R. acutus* are serrated in adults (Compagno, 1984). In our specimens, the serrations are absent, indicating immature individuals. Distinguishing between the teeth of *R. acutus* and *R. oligolinx* is difficult, where both have very fine irregular serrations. However, due to questionable distribution of *R. oligolinxi* in Taiwan (Ebert et al., 2013; Froese & Pauly, 2022), we tentatively assign these specimens to *R. acutus*.

Family Galeocerdonidae *sensu* Ebersole, Cicimurri & Stringer, 2019

Genus *Galeocerdo* Müller & Henle, 1837

Galeocerdo cuvier (Péron & Lesueur, 1822)

(Fig. 17A–C)

?1965 *Galeocerdo aduncus*; Huang, pl. 22, figs. 10, 11.

?1978 *Galeocerdo aduncus*; Uyeno, pl. 1, fig. 3.

2004 Elasmobranchii indet.; Xue, pl. 6, figs. 1–7, pl. 8, fig. 6.

Referred specimens: n = 7: ASIZF0100459, CMM F0213, F0215, F0245, F2823, F2829, NTM I01121.

Description: CH = 12.27–17.72 mm; MCL = 17.37–26.88 mm; BCW = 18.10–28.05 mm. The teeth of *G.cuvier* are characterized by a coarsely serrated crown with a cusp that strongly curves distally and a prominent distal heel demarcated by a deep notch at approximately 90 degrees angle along the distal cutting edge. Fine secondary serrations are present on the coarser primary serrations. The serrations on the distal heel in ASIZF0100459 (Fig. 17B) are pathologically formed weakly, where its mesiodistally wide tooth suggests that it is a distal tooth. CMM F0245 and CMM F0215 are mesial teeth with well-marked serration (Fig. 17A, C).

Remarks: Five extinct species and one extant species of *Galeocerdo* are considered valid: the Eocene †*G. clarkensis* and †*G. eaglesomei*, Oligocene–late Miocene †*G. aduncus*, Miocene †*G. mayumbensis*, Pliocene †*G. capellini*, and the Pleistocene–Recent *G. cuvier* (Purdy et al., 2001;

Türtscher et al., 2021). Huang (1965) reported a questionable occurrence of †*G. aduncus* from the Pleistocene Cholan Formation in Hsinchu, northern Taiwan, which we consider the specimen is lost. Uyeno (1978) reported another occurrence of †*G. aduncus* from the poorly constrained Plio-Pleistocene strata along the Tsailiao River in Tainan, southwestern Taiwan (as Miocene to Pleistocene in Uyeno, 1978). Although Uyeno's collection was deposited in the NTM, we were not able to locate the specimen of †*G. aduncus* in the collection. Nevertheless, although the whereabouts of their specimen is uncertain, they are interpreted here to have also belonged to *G. cuvier*.

Family Sphyrnidae Bonaparte, 1840
Genus *Sphyrna* Rafinesque, 1810
Sphyrna lewini (Griffith & Smith, 1834)
(Fig. 17D)

?1978 *Sphyrna* sp.; Uyeno, pl. 2, fig. 8

Referred specimens: n = 2: CMM F0235, F0312.
Description: CH = 6.85 mm; MCL = 11.17 mm; BCW = 10.53 mm. The tooth crown of *S. lewini* is characterized by a slender distally inclined cusp with a narrow, mesially extended base demarcated by a slight concavity song the mesial cutting edge and a low distal heel demarcated by a deep notch. Both cutting edges are smooth without serrations. The root is low, and its base is straight. It has a deep nutritive groove on the lingual side and extends to the root base.
Remarks: The teeth of *Sphyrna lewini* are most similar to *S. macrorhynchos* and *Loxodon macrorhinus*, but a slight concavity is present on the base of the mesial cutting edge in *S. lewini*, whereas the edge is almost straight in the latter two species (Ebert et al., 2013).

Order Myliobatiformes Compagno, 1973
Family Dasyatidae Jordan & Gilbert, 1879
Genus *Dasyatis* Rafinesque, 1810
Dasyatis sp.
(Fig. 18)

1978 *Dasyatis* sp.; Uyeno, pl. 4, figs. 25, 26.

Referred specimens: n = 2: ASIZF0100590, 0100591.
Description: The specimens are roughly hexagonal with a globular, thick crown and a well-divided bilobed root that is smaller than the crown and extends ventrally. The apex of the crown in both specimens is flat, but the specimen ASIZF0100590 (Fig. 18A) has blunt, rounded corners compared to ASIZF0100591 (Fig. 18B).

Remarks: The teeth of *Dasystis* are highly variable, where some species even exhibits sexual dimorphism (Kajiura & Tricas, 1996, and references therein). The teeth of females and juvenile males are more quadrangular and rounded, with flat crowns and blunt corners. They have a central ridge that separates the labial and lingual surfaces. The mature males, however, have teeth with triangular and high cusps and retain the pitted ornamentation on the labial face (Kajiura & Tricas, 1996; Taniuchi & Shimizu, 1993).

Family Aetobatidae Agassiz, 1858
Genus *Aetobatus* Blainville, 1816
Aetobatus ocellatus (Kuhl, 1823)
(Fig. 19)

Referred specimens: n = 58: ASIZF0100549–0100580, CMM F0380, F0382, F0388, F0395, F0399–0409, F0412, F2848–F2850, F2852–F2854, NTM I01116, I01117, I01119, I01120.
Description: Teeth of *Aetobatus* are characterized by strongly extended roots on the lingual (posterior) side and the arcuate crown in apical view with a flat occlusal surface. The crown overhangs the root on the labial (anterior) side and the root is more prominent than the crown on the lingual side. Both lingual and labial crown faces have fine vertical grooves as ornamentations. The root is polyaulocorhizous, consisting of anteroposteriorly oriented, densely packed, vertical lamellar plates.
Remarks: See remarks under *Myliobatis tobijei*.

Family Myliobatidae Bonaparte, 1835
Genus *Myliobatis* Cuvier, 1816
Myliobatis tobijei Bleeker, 1854
(Fig. 20)

Referred specimens: n = 29: ASIZF0100581–0100589, CMM F0378, CMM F0379, F0381, F0383–F0387, F0389–F0393, F0394, F0396–F0398, F0410, F0411, F2855, NTM I01118.
Description: Each tooth of *Myliobatis* has a flat occlusal surface and is laterally elongated and hexagonal that may be straight or slightly arched. The root is polyaulocorhizous with well-defined anteroposteriorly oriented, vertical lamellar plates separated by deep grooves, where the crown overhangs the root on the labial (anterior) face. The lingual and labial faces are ornamented with a network of fine reticulated ridges that grade into longitudinal ridges in the apical and become finer and anastomotic.
Remarks: The tooth plates of *Myliobatis* are similar to those of *Aetomylaeus* and *Aetobatus*, but the lateral angle of the hexagonal tooth plates in *Aetomylaeus* is more oblique than that of *Myliobatis* (Ebersole, Cicimurri & Stringer, 2019). The vertical lamellar plates of the root in *Myliobatis* are coarser than *Aetobatus*. Teeth of *Myliobatis* lack the tuberculated enameloid on

the occlusal surface, whereas teeth of *Aetomylaeus* are reticulated on the labial and lingual faces (Ebersole, Cicimurri & Stringer, 2019).

Discussion

Previous works on fossil elasmobranchs in Taiwan are very scarce, where they were limited in scope often lacked formal description, and were mostly not based on specimens in museum repositories (Lin et al., 2021). Huang (1965) reported three shark taxa while describing a fossil whale tympanic bone from the early Pleistocene Cholan Formation in northern Taiwan (as early Pliocene in Huang, 1965). Although the whereabouts of the specimens are unknown, it is one of the earliest accounts reporting fossil shark teeth in Taiwan. Uyeno (1978) listed nine elasmobranch taxa from the Pleistocene Chochen–Tsailiao area with images of the specimens but without descriptions, and while accessible, these materials are reviewed here.

Perhaps the most complete description on a single fossil shark assemblage in Taiwan is the one by Tao & Hu (2008) from the late Miocene Tangenshan Sandstone Formation in Chiahsien County, Kaohsiung. They described five taxa common in late Miocene marine deposits (*Otodus megalodon*, *Odontaspis* sp., †*Isurus hastalis*, †*Hemipristis serra*, and *Carcharhinus* sp.) as well as a new extinct species of *Hemipristis*, *H. liui* Tao & Hu, 2008. The specimen of *H. liui* is an upper tooth and is characterized by asymmetric serrations on the distal and mesial cutting edges. On the other hand, the occurrences of *O. megalodon* are mentioned sparsely in Taiwan (Hu & Tao, 1993; Tao & Hu, 2008) and likely available in the private collections, which are potentially one of the directions for future research efforts (Haug et al., 2020; Lin et al., 2021).

The 697 elasmobranch teeth from the Liuchungchi Formation in Niubu described in this study reveal the presence of at least 23 elasmobranch taxa (Table 1). The majority of our specimens are well-preserved with almost no evidence of significant erosion or weathering, indicating that postmortem transportation was minimal. The excellent overall preservation allowed species-level taxonomic identification for most of the specimens, which in turn, permitted the elucidation of the diverse elasmobranch community. In fact, the assemblage represents the most diverse elasmobranch paleofauna from Taiwan reported to date.

The materials were mainly based on surface collecting that span over more than three decades, and we note that our bulk sediment samples (weighing up to 830 kg) only yield three specimens (ASIZF0100548, ASIZF0100590, ASIZF0100591). Surface collecting likely results in sampling bias towards larger specimens underrepresenting smaller specimens (Welton & Farish, 1993; Perez, 2022). Nevertheless, the high diversity captured in our study is significant in the spatio-temporal context. For example, *Carcharodon carcharias* is only distributed in today's southern, eastern, and northeastern Taiwan, but not in the west coast where the fossils were found (Teng, 1958; Shen, 1993; Ebert et al., 2013; Shao, 2022). According to the Fisheries Agency, Council of Agriculture, Taiwan (Taiwan Fisheries Agency, 2021), a total of 39 individuals of *C. carcharias* were caught between 2012 and 2021, with the majority of landings in northeastern Taiwan. However, in our fossil sites, teeth of *C. carcharias* are the second most abundant, where the largest anterior tooth specimen in our study (ASIZF0100340, with a crown height of 41.03 mm) is estimated to have come from an individual that measured about 4.8–4.9 m in total length (see Shimada, 2002a; Adnet et al., 2009), which must have been a mature, large individual (Ebert et al., 2013).

One of the most noteworthy occurrences reported in this study is that of the extinct species †*Hemipristis serra*. The species is known worldwide, but most of the documented occurrences are from the Miocene and Pliocene deposits (e.g., Yabumoto & Uyeno, 1994; Sánchez-Villagra et al., 2000; Marsili et al., 2007; Portell et al., 2008; Visaggi & Godfrey, 2010; Carrillo-Briceño et al., 2015). The fossil record indicates that the fossil species preferred in warm neritic environments (Cappetta, 2004, 2012). Although most previous studies suggest its last appearance at the end of the Pliocene, new evidence indicates that †*H. serra* persisted through the Pleistocene in North America (Ebersole, Ebersole & Cicimurri, 2017; Boessenecker, Boessenecker & Geisler, 2018; Perez, 2022). Previous records of †*H. serra* from Taiwan are that reported by Uyeno (1978) from an uncertain stratigraphic horizon along Tsailiao River, and that by Tao & Hu (2008) from the Miocene Kueichulin Formation in southern Taiwan. The †*H. serra* specimens described here are the first confirmed Pleistocene record in Taiwan as well as in the entire Northwest Pacific, meaning that the North American population was not a local survivor. It should be noted that the preservation of all three specimens of †*H. serra* described in this study are excellent (Fig. 6B–D), and thus they most certainly do not represent fossils derived from an older horizon.

The assemblage is numerically dominated by two genera, *Carcharhinus* (Carcharhinidae, n = 462) and *Carcharodon* (Lamnidae, n = 52), comprising more than 77.5% of the total specimen count and about half of the taxa identified (11 out of 24). From a paleoecological perspective, the composition is roughly similar to the one found in modern western Taiwan (Ebert et al., 2013; Shao, 2022). For example, the most abundant species of *Carcharhinus* in this study, *C. leucas*, presently lives close to the coastal area of tropical and subtropical riverine and lacustrine (Compagno, 1984). The second abundant species in this study, *Carcharodon carcharias*, inhabits inshore shallow water to open ocean and, as a top predator, feeds on larger marine mammals and fishes (Ebert et al., 2013; Compagno, 2002). While pelagic sharks *Carcharhinus plumbeus* and *C. longimanus* are also frequently represented in the Pleistocene assemblage, the occurrences of *C. altimus*, *Myliobatis tobijei*, and *Aetobatus ocellatus* may suggest possible presence of deeper sandy, flat bottoms (Compagno, 1984). The abundant associated marine vertebrate fossils, such as bony fish bones (Tao, 1993) and otoliths (Lin et al., 2018) as well as whale bones (Xue, 2004), indicate a rich, thriving marine ecosystem in the area. The sedimentary environment of the Liuchungchi Formation further points to shoreface to inner offshore setting, with several transgression and regression cycles (Chen, 2016). Taken together, an inshore to offshore shallow-water environment with sandy bottoms can be interpreted for coastal areas in southwest Taiwan during the early Pleistocene.

Conclusions

Fossil fish fauna from the tropical-subtropical West Pacific is poorly known compared to its modern analog, impeding our understanding of the formation of this current marine biodiversity hotspot. Using elasmobranch fossils from an early Pleistocene locality in southern Taiwan, we report a previously unnoticed but highly diverse shark and ray fauna from the region. The taxonomic composition of the assemblage reveals a nearshore shallow-water paleoenvironment and agrees with sedimentary interpretation. In addition, the presence of †*Hemipristis serra* and large specimens of *Carcharodon carcharias* highlight the potential for similar studies from other strata and localities, which would allow a more comprehensive picture of the evolutionary history and biogeographic distribution of the species. The present study can be regarded as the most extensive on elasmobranch fossils from Taiwan.

Acknowledgements

We would like to express our sincere gratitude to Prof. Hsi-Jen Tao (National Taiwan University) who donated the specimens to the Biodiversity Research Museum, Academia Sinica, Taiwan. We also thank Mrs. Hsiao I-Ju (Chiayi Municipal Museum, CMM) for her administrative assistance in examining the CMM collection, and Miss Sun You-Yu (National Taiwan Museum) for accessing the collection described by Uyeno (1978).

References

Adnet S, Balbino AC, Antunes MT, Marín-Ferrer JM. 2009. New fossil teeth of the White Shark (*Carcharodon carcharias*) from the Early Pliocene of Spain. Implication for its paleoecology in the Mediterranean. *Neues Jahrbuch für Geologie und Paläontologie Abhandlungen* 256/1: 7–16 DOI: 10.1127/0077-7749/2009/0029.

Boessenecker SJ, Boessenecker RW, Geisler JH. 2018. Youngest record of the extinct walrus *Ontocetus emmonsi* from the Early Pleistocene of South Carolina and a review of North Atlantic walrus biochronology. *Acta Palaeontologica Polonica* 63: 279–286 DOI: 10.4202/app.00454.2018.

Buckeridge JS, Chan BK, Lee S-W. 2018. Accumulations of fossils of the whale barnacle *Coronula bifida* Bronn, 1831 (Thoracica: coronulidae) provides evidence of a Late Pliocene cetacean migration route through the Straits of Taiwan. *Zoological Studies* 57: 1–12

Carrillo-Briceñoa JD, De Gracia C, Pimiento C, Aguilera OA, Kindlimann K, Santamarina P, Jaramillo C. 2015. A new Late Miocene chondrichthyan assemblage from the Chagres Formation, Panama. *Journal of South American Earth Sciences* 60: 56–70 DOI: 10.1016/j.jsames.2015.02.001

Cappetta H. 2004. *Handbook of Paleoichthyology, Vol. 3B: Condrichthyes II Mesozoic and*

Cenozoic Elasmobranchii. Müchen: Verlag Dr Friedrich Pfeil.

Cappetta H. 2012. *Handbook of Paleoichthyology, Vol. 3E: Chondrichthyes Mesozoic and Cenozoic Elasmobranchii: Teeth.* Müchen: Verlag Dr Friedrich Pfeil.

Chen W-S. 2016. *An introduction to the geology of Taiwan*. Taipei: Geological Society of Taiwan.

Chen W-S, Huang N-E, Yang C-C. 2011. Pleistocene sequence stratigraphic characteristics and foreland basin evolution, southwestern Taiwan. *Special Publication of the Central Geological Survey* 25: 1–28

Chou J-T. 1975. A sedimentologic study of the Miocene Pachangchi Sandstone in the Chiayi region, Western Taiwan. *Petroleum Geology of Taiwan* 12: 81–96

Compagno LJV. 1984. *FAO species catalogue. Sharks of the World: An Annotated and Illustrated Catalogue of Shark Species Known To Date, Volume 4: Carcharhiniformes.* Rome: Food and Agriculture Organization of the United Nations.

Compagno LJV. 1988. *Sharks of the Order Carcharhiniformes.* New Jersey: Princeton University Press.

Compagno, LJV. 2002. *FAO species catalogue. Sharks of the World: An Annotated and Illustrated Catalogue of Shark Species Known To Date, Volume 2: Bullhead, Mackerel and Carpet Sharks (Heterodontiformes, Lamniformes and Orectolobiormes).* Rome: Food and Agriculture Organization of the United Nations.

Covey M. 1984. Lithofacies analysis and basin reconstruction, Pio-Pleistocene western Taiwan foredeep. *Petroleum Geology of Taiwan* 20: 53–83

Ebersole JA, Ebersole SM, Cicimurri DJ. 2017. The occurrence of early Pleistocene marine fish remains from the Gulf Coast of Mobile County, Alabama, USA. *Palaeodiversity* 10: 97–115 DOI: 10.18476/pale.v10.a6.

Ebersole JA, Cicimurri DJ, Stringer GL. 2019. Taxonomy and biostratigraphy of the elasmobranchs and bony fishes (Chondrichthyes and Osteichthyes) of the lower-to-middle Eocene (Ypresian to Bartonian) Claiborne Group in Alabama, USA, including an analysis of otoliths. *European Journal of Taxonomy* 585: 1–274.

Ebert DA, White WT, Ho H-C, Last PR, Nakaya K, Seret B, Straube N, Naylor GJP, De Carvalho MR. 2013. An annotated checklist of the chondrichthyans of Taiwan. *Zootaxa* 3752: 279–386

Ebert DA, Dando M, Fowler S. 2021. *Shark of the world, A complete guide.* New Jersey: Princeton University Press.

Ehret DJ, Macfadden BJ, Jones DS, Devries TJ, Foster DA, Salas-Gismondi R. 2012. Origin of the white shark *Carcharodon* (Lamniformes: Lamnidae) based on recalibration of the Upper Neogene Pisco Formation of Peru. *Palaeontology* 55: 1139–1153 DOI: 10.1111/j.1475-4983.2012.01201.x.

Fricke R, Eschmeyer WN, Van der Laan R, eds. 2022. Eschmeyer's SCHMEYER'S CATALOG OF FISHES: GENERA, SPECIES, REFERENCES, version 02/2022, *Available at http://researcharchive.calacademy.org/research/ichthyology/catalog/fishcatmain.asp* (accessed May 2022).

Froese R, Pauly D, eds. 2022. FishBase. World Wide Web electronic publication. www.fishbase.org, version 02/2022, *Available at https://www.fishbase.se/search.php* (accessed May 2022).

Ho C-S. 1967. Foothill tectonics of Taiwan. *Bulletin of the Geological Survey of Taiwan* 25: 9–28

Ho C-S. 1976. Structural evolution of Taiwan, *Tectonophysics* 4: 367–378

Hu C-H. 1989. Manual for ten geological routes in central Taiwan—route 7: geology along the Nanheng Highway—Tsailiao, Peiliao, Chiahsien. In: Faculty members of the Department of Earth Sciences, National Taiwan Normal University, editors. *Field manual of the geology of Taiwan (II).* Taipei: Department of Earth Sciences, National Taiwan Normal University, 105–163

Hu C-H, Tao H-J. 1993. *The fossil faunas of Penghu Islands, Taiwan.* Penghu: Penghu District Cultural Center Publications.

Haug C, Reumer JWF, Haug JT, et al. 2020. Comment on the letter of the Society of Vertebrate Paleontology (SVP) dated April 21, 2020 regarding "Fossils from conflict zones and reproducibility of fossil-based scientific data": the importance of private collections. *Paläontologische Zeitschrift* 94: 413–429 DOI: 10.1007/s12542-020-00522-x.

Huang T. 1965. A new species of a whale tympanic bone from Taiwan, China. *Transaction and Proceedings of the Palaeonotological Society of Japan* 61: 183–187

Huang W-C. 2010. Stratigraphic sequences in distal part of foreland Basin in Southwestern Taiwan: Model of interplay between tectonics and eustasy. Master Thesis, Department of Earth Sciences, National Cheng Kung University.

Kajiura SM, Tricas T. 1996. Seasonal dynamics of dental dimorphism in the Atlantic Stingray *Dasyatis sabina*. *Journal of Experimental Biology* 199: 2297-306

Lin C-H, Chien C-W. 2022. Late Miocene otoliths from northern Taiwan: insights into the rarely known Neogene coastal fish community of the subtropical northwest Pacific. *Historical Biology* 34: 361–382 DOI: 10.1080/08912963.2021.1916012

Lin C-H, Chien C-W, Lee S-W, Chang C-W. 2021. Fossil fishes of Taiwan, a review and prospection. *Historical Biology* 33: 1362–1372 DOI: 10.1080/08912963.2019.1698563.

Lin C-H, Ou H-Y, Lin C-Y, Chen H-M. 2022. First skeletal fossil record of the red seabream *Pagrus major* (Sparidae, Perciformes) from the Late Pleistocene of subtropical West Pacific, southern Taiwan. *Zoological Studies* 61: 10 DOI: 10.6620/ZS.2022.61-10

Lin C-H, Wang L-C, Wang C-H, Chang C-W. 2018. Common early Pleistocene fish otoliths from Niubu in Chia-Yi County, southwestern Taiwan. *Journal of the National Taiwan Museum* 71: 47–68 DOI: 10.6532/JNTM.201809_71(3).04.

Lin A-T, Watts AB. 2002. Origin of the west Taiwan basin by orogenic loading and flexure of a rifted continental margin. *Journal of Geophysical Research* 107: 2185.

Lundberg N, Reed DL, Liu C-S, Lieske J. 1997. Forearc-basin closure and arc accretion in the submarine suture zone south of Taiwan. *Tectonophysics* 274: 5–23.

Marsili S, 2006. Revision of the teeth of the genus *Carcharhinus* (Elasmobranchii; Carcharhinidae) from the Pliocene of tuscany, Italy. *Rivista Italiana di Paleontologia e Stratigrafia* 113: 79–95 DOI: 10.13130/2039-4942/6360.

Marsili S, Carnevale G, Danese E, Bianucci G, Landini W. 2007. Early Miocene vertebrates from Montagna della Maiella, Italy. *Annales de Paléontologie* 93: 1, 27-66 DOI: 10.1016/j.annpal.2007.01.001.

Nagel S, Castelltort S, Wetzel A, Willett SD, Mouthereau F, Lin A-T. 2013. Sedimentology and foreland basin paleogeography during Taiwan arc continent collision. *Journal of Asian Earth Sciences* 62: 180–204.

Nelson JS, Grande TC, Wilson MVH. 2016. *Fishes of the world.* New Jersey: John Wiley & Sons.

Naylor GJP, Marcus LF. 1994. Identifying isolated shark teeth of the genus *Carcharhinus* to species relevance for tracking phyletic change through the fossil record. *American Museum Novitates* 3109: 56

Perez VJ. 2022. The chondrichthyan fossil record of the Florida Platform (Eocene–Pleistocene). *Paleobiology* DOI: 10.1017/pab.2021.47.

Portell RW, Hubbell G, Donovan SK, Green JL, Harper DAT, Pickerill R. 2008. Miocene sharks in the Kendeace and Grand Bay formations of Carriacou, The Grenadines, Lesser Antilles. *Caribbean Journal of Science* 44: 279–286 DOI: 10.18475/cjos.v44i3.a2.

Purdy RW, Schneider VP, Applegate SP, McLellan JH, Meyer RL, Slaughter BH. 2001. The Neogene sharks, rays, and bony fishes from Lee Creek Mine, Aurora, North Carolina. In Ray CE, Bohaska DH, *Geology and Paleontology of the Lee Creek Mine, North Carolina, III: Smithsonian Contributions to Paleobiology*. Washington: Smithsonian Institution Press, 71–160.

Purdy RW. 2006. A Key to Common Genera of Neogene Shark Teeth. *Available at http://paleobiology.si.edu/pdfs/sharktoothKey.pdf* (accessed May 2022).

Ribas-Deulofeu L, Wang Y-C, Lin C-H. 2021. First record of Late Miocene *Dendrophyllia* de Blainville, 1830 (Scleractinia: Dendrophylliidae) in Taiwan. *Terrestrial, Atmospheric and Oceanic Sciences* 32: 1061–1068 DOI: 10.3319/TAO.2021.09.13.02

Sánchez-Villagra MR, Burnham RJ, Campbell DC, Feldmann RM, Gaffney ES, Kay RF, Lozsan R, Purdy R, Thewissen JGM. 2000. A new near-shore marine fauna and flora from the Early Neogene of northwestern Venezuela. *Journal of Paleontology* 74: 957–968 DOI:10.1017/s0022336000033126.

Shao K-T. 2022. Taiwan Fish Database. WWW Web electronic publication. *Available at http://fishdb.sinica.edu.tw* (accessed May 2022).

Shen S-C. 1993. *Fishes of Taiwan*. Taipei: Department of Zoology, National Taiwan University.

Shimada K. 2002a. The relationship between the tooth size and total body length in the white shark, *Carcharodon carcharias*. *Journal of Fossil Research* 35: 28–33

Shimada K. 2002b. Dental Homologies in Lamniform Sharks (Chondrichthyes: Elasmobranchii). *Journal of Morphology* 251:38–72

Smith JLB. 1957. The rare shark *Hemipristis elongatus* (Klunzinger), 1871, from Zanzibar and Mozambique. *Annals and Magazine of Natural History* 10: 555-560 DOI: 10.1080/00222935708655997.

Stach L-W. 1957. Stratigraphic subdivision and correlation of the upper Cenozoic sequence in the foothills region east of Chiayi and Hsinying, Taiwan, China. *Symposium on Petroleum Geology of Taiwan*, 177–230.

Suppe J. 1984. Kinematics of arc-continent collision, flipping of subduction, and back-arc spreading near Taiwan. *Journal of the Geological Society of China* 6: 21–33.

Taiwan Fisheries Agency. 2021. Coastal Great White Sharks, Megamouth Sharks, Elephant Sharks, Manta Rays Reported Statistics. Fisheries Agency, Taipei, Taiwan.

Taniuchi T, Shimizu M. 1993. Dental sexual dimorphism and food habits in the stingray Dasyatis akajei from Tokyo Bay, Japan. *Nippon Suisan Gakkaishi* 59: 53–60.

Tao H-J. 1993. A new Miocene fossil species *Priacanthus liui* (Pisces: perciformes) from the Nanchung Formation in Chiayi Hsien, Taiwan. *Bulletin of the National Museum of Nature and Science* 4: 91–100.

Tao H-J, Hu C-H. 2008. Fossil chondrichthyes fishes of Chia-hsien, Kaoshung County, Taiwan. *Journal of the National Taiwan Museum* 61: 41–62.

Teng H-T. 1958. Studies on the elasmobranch fishes from Formosa. Part 1. Eighteen unrecorded species of sharks from Formosa. *Reports of the Laboratory of Fishery Biology, Taiwan Fisheries Research Institute* 3: 1–30.

Teng L-S. 1990. Geotectonic evolution of late Cenozoic arc-continent collision in Taiwan. *Tecionophysics* 183: 57–76.

Türtscher J, López-Romero FA, Jambura PL, Kindlimann R, Ward DJ, Kriwet J. 2021. Evolution, diversity, and disparity of the tiger shark lineage *Galeocerdo* in deep time. *Paleobiology* 47: 574–590 DOI: 10.1017/pab.2021.6.

Uyeno T. 1978. A preliminary report on fossil fishes from Ts'o-chen Tainan. *Science Report Geology and Paleontology* 1: 5–17

Visaggi CC, Godfrey SJ. 2010. Variation in composition and abundance of Miocene shark teeth from Calvert Cliffs, Maryland. *Journal of Vertebrate Paleontology* 30: 26–35 DOI: 10.1080/02724630903409063.

Voigt M, Weber D. 2011. *Field guide for sharks of the genus Carcharhinus.* München: Verlag Dr. Friedrich Pfeil.

Weigmann S. 2016. Annotated checklist of the living sharks, batoids and chimaeras (Chondrichthyes) of the world, with a focus on biogeographical diversity. *Journal of Fish Biology* 88: 837–1037 DOI: 10.1111/jfb.12874.

Welton BJ, Farish RF. 1993. The collector's guide to Fossil Sharks and Rays from the Cretaceous of Texas. Lewisville, Texas: Before Time.

White WT. 2012. A redescription of *Carcharhinus dussumieri* and *C. sealei*, with resurrection of *C. coatesi* and *C. tjutjot* as valid species (Chondrichthyes Carcharhinidae). *Zootaxa* 3241: 1–34.

Whitenack LB, Gottfried MD. 2010. A morphometric approach for addressing tooth-based species delimitation in fossil mako sharks, *Isurus* (Elasmobranchii: Lamniformes). *Journal of Vertebrate Paleontology* 30: 17–25 DOI: 10.1080/02724630903409055.

Wilmers J, Waldron M, Bargmann S. 2021. Hierarchical microstructure of tooth enameloid in two Lamniform shark species, *Carcharias taurus* and *Isurus oxyrinchus*. *Nanomaterials* 11: 969 DOI: 10.3390/nano11040969.

Xue W-J. 2004. *Chiayi area fossil map.* Chiayi: Chiayi City Cultural Bureau.

Yabumoto Y, Uyeno T. 1994. Late Mesozoic and Cenozoic fish faunas of Japan. *Island Arc* 3: 255-269 DOI: 10.1111/j.1440-1738.1994.tb00115.x.

Yu H-S, Chou Y-W. 2001. Characteristics and development of the flexural forebulge and basal unconformity of Western Taiwan Foreland Basin. *Tectonophysics* 333: 277–291

Supplemental file

Supplemental Figure S1. Aerial photographs of the Niubu locality showing the closest sampling site to the weir (red square, Site 1 in Fig. 2B). A, general view; B, C, closer views of the sampling site.

Figure captions

Figure 1. Summary of the sampling sites. A, overview of geological map of Taiwan (modified after Chen, 2016). B, geological map of Nuibu area, Chiayi (map extracted from National Geological Data Warehouse, Central Geological Survey, MOEA). Yellow stars = sampling sites (see Fig. 2B for details). C, stratigraphic correlation of the Western Foothills (modified after Chen, 2016). The examined Liuchungchi Formation is indicated in red.

Figure 2. A, stratigraphic column (modified after Huang, 2010). B, details of the sampling sites. GPS coordinates: Site 1 = 23°26'23.4"N, 120°35'35.5"E; Site 2 = 23°26'22.6"N, 120°35'32.7"E; Site 3 = 23°26'23.5"N, 120°35'29.8"E.

Figure 3. Shark teeth from the early Pleistocene of Liuchungchi Formation of Niubu, southern Taiwan. A, B, *Carcharias taurus*; A, ASIZF0100320; B, CMM F0204. C, *Alopias vulpinus*, ASIZF0100532. Scale bars = 1 cm. 1 = lingual view; 2 = labial view; 3 = lateral view.

Figure 4. *Carcharodon carcharias* teeth from the early Pleistocene of Liuchungchi Formation of Niubu, southern Taiwan. A, ASIZF0100344; B, ASIZF0100337; C, ASIZF0100338; D, ASIZF0100336; E, ASIZF0100335; F, ASIZF0100339; G, ASIZF0100340; H, ASIZF0100324;

I, ASIZF0100328; J, ASIZF0100325; K, ASIZF0100326; L, ASIZF0100323. Scale bar = 1 cm. 1 = lingual view; 2 = labial view.

Figure 5. *Isurus oxyrinchus* teeth from the early Pleistocene of Liuchungchi Formation of Niubu, southern Taiwan. A, ASIZF0100317; B, ASIZF0100318; C, ASIZF0100321; D, CMM F0242. Scale bar = 1 cm. 1 = lingual view; 2 = labial view; 3 = lateral view.

Figure 6. Shark teeth from the early Pleistocene of Liuchungchi Formation of Niubu, southern Taiwan. A, *Hemipristis elongata*, CMM F0232. B–D, †*Hemipristis serra*; B, ASIZF0100460; C, ASIZF0100461; D, ASIZF0100462. Scale bars = 1 cm. 1 = lingual view; 2 = labial view.

Figure 7. *Carcharhinus altimus* teeth from the early Pleistocene of Liuchungchi Formation of Niubu, southern Taiwan. A, ASIZF0100357; B, ASIZF0100359; C, CMM F0363; D, CMM F0293; E, CMM F0322; F, ASIZF 0100365. Scale bar = 1 cm. 1 = lingual view; 2 = labial view.

Figure 8. *Carcharhinus amboinensis* teeth from the early Pleistocene of Liuchungchi Formation of Niubu, southern Taiwan. A, ASIZF 0100419; B, ASIZF0100368, C, ASIZF0100425; D, ASIZF0100366; E, CMM F0209; F, ASIZF0100369. Scale bar = 1 cm. 1 = lingual view; 2 = labial view.

Figure 9. *Carcharhinus leucas* teeth from the early Pleistocene of Liuchungchi Formation of Niubu, southern Taiwan. A, ASIZF0100398; B, ASIZF0100397; C, ASIZF0100394; D, ASIZF0100411; E, ASIZF0100396; F, ASIZF 0100395, G, ASIZF0100400; H, ASIZF0100402; I, ASIZF0100390. Scale bar = 1 cm. 1 = lingual view; 2 = labial view.

Figure 10. *Carcharhinus limbatus* teeth from the early Pleistocene of Liuchungchi Formation of Niubu, southern Taiwan. A, ASIZF0100470; B, ASIZF0100476; C, ASIZF0100469; D, ASIZF0100468; E, CMM F0236; F, CMM F0111; G, CMM F0237; H, CMM F0238. Scale bar = 1 cm. 1 = lingual view; 2 = labial view.

Figure 11. *Carcharhinus longimanus* teeth from the early Pleistocene of Liuchungchi Formation of Niubu, southern Taiwan. A, ASIZF 0100371; B, ASIZF0100376; C, ASIZF0100370; D, ASIZF0100377; E, ASIZF0100375; F, ASIZF0100378; G, ASIZF0100374; H, ASIZF0100373; I, ASIZF0100392; J, ASIZF0100391. Scale bar = 1 cm. 1 = lingual view; 2 = labial view.

Figure 12. *Carcharhinus obscurus* teeth from the early Pleistocene of Liuchungchi Formation of Niubu, southern Taiwan. A, ASIZF0100372; B, ASIZF0100384; C, ASIZF0100385; D, ASIZF0100386; E, ASIZF0100388; F, ASIZF0100387; G, ASIZF0100383. Scale bar = 1 cm. 1 = lingual view; 2 = labial view.

Figure 13. *Carcharhinus plumbeus* teeth from the early Pleistocene of Liuchungchi Formation of Niubu, southern Taiwan. A, ASIZF0100412; B, ASIZF0100406; C, ASIZF0100405; D, ASIZF0100410; E, ASIZF0100409; F, ASIZF0100408; G, ASIZF0100407. Scale bar = 1 cm. 1 = lingual view; 2 = labial view.

Figure 14. *Carcharhinus sorrah* teeth from the early Pleistocene of Liuchungchi Formation of Niubu, southern Taiwan. A, CMM F0129; B, CMM F0119; C, ASIZF0100418; D, CMM F0126; E, CMM F0135; F, CMM F0122; G, CMM F0140. Scale bar = 1 cm. 1 = lingual view; 2 = labial view.

Figure 15. *Carcharhinus tjutjot* teeth from the early Pleistocene of Liuchungchi Formation of Niubu, southern Taiwan. A, ASIZF0100415; B, ASIZF0100414; C, CMM F0116; D, ASIZF0100413; E, ASIZF0100417; F, ASIZF0100416; G, CMM F0323; H, CMM F0324. Scale bar = 1 cm. 1 = lingual view; 2 = labial view.

Figure 16. Shark teeth from the early Pleistocene of Liuchungchi Formation of Niubu, southern Taiwan. A–C, *Negaprion acutidens*; A, ASIZF0100533; B, ASIZF0100531; C, CMM F0203. D–H, *Rhizoprionodon acutus*; D, ASIZF0100463; E, CMM F0120; F, CMM F0131; G, CMM F0121; H, ASIZF0100464. Scale bar = 1 cm. 1 = lingual view; 2 = labial view.

Figure 17. Shark teeth from the early Pleistocene of Liuchungchi Formation of Niubu, southern Taiwan. A–C, *Galeocerdo cuvier*; A, CMM F0215; B, ASIZF0100459; C, CMM F0245. D, *Sphyrna lewini*, CMM F0235. Scale bars = 1 cm. 1 = lingual view; 2 = labial view.

Figure 18. *Dasyatis* sp. teeth from the early Pleistocene of Liuchungchi Formation of Niubu, southern Taiwan. A, ASIZF0100590; B, ASIZF0100591. Scale bar = 5 mm. 1 = occlusal view; 2 = basal view; 3 = lingual view; 4 = lateral view.

Figure 19. *Aetobatus ocellatus* teeth from the early Pleistocene of Liuchungchi Formation of Niubu, southern Taiwan. A, CMM F2854; B, CMM F2850; C, CMM F0408; D, ASIZF0100549. Scale bar = 1 cm. 1 = occlusal view; 2 = basal view.

Figure 20. *Myliobatis tobijei* teeth from the early Pleistocene of Liuchungchi Formation of Niubu, southern Taiwan. A, ASIZF0100582; B, ASIZF0100587; C, ASIZF0100586; D, CMM F0395; E, CMM F2855; F, CMM F0393; G, CMM F0398. Scale bars = 1 cm. 1 = occlusal view; 2 = basal view; 3 = lingual view; 4 = lateral view.

Table captions

Table 1. Elasmobranch from the early Pleistocene Liuchungchi Formation, Chiayi, southern Taiwan.

Figure 1

Summary of the sampling sites.

A, overview of geological map of Taiwan (modified after Chen, 2016). B, geological map of Nuibu area, Chiayi (map extracted from National Geological Data Warehouse, Central Geological Survey, MOEA). Yellow stars = sampling sites (see Fig. 2B for details). C, stratigraphic correlation of the Western Foothills (modified after Chen, 2016). The examined Liuchungchi Formation is indicated in red.

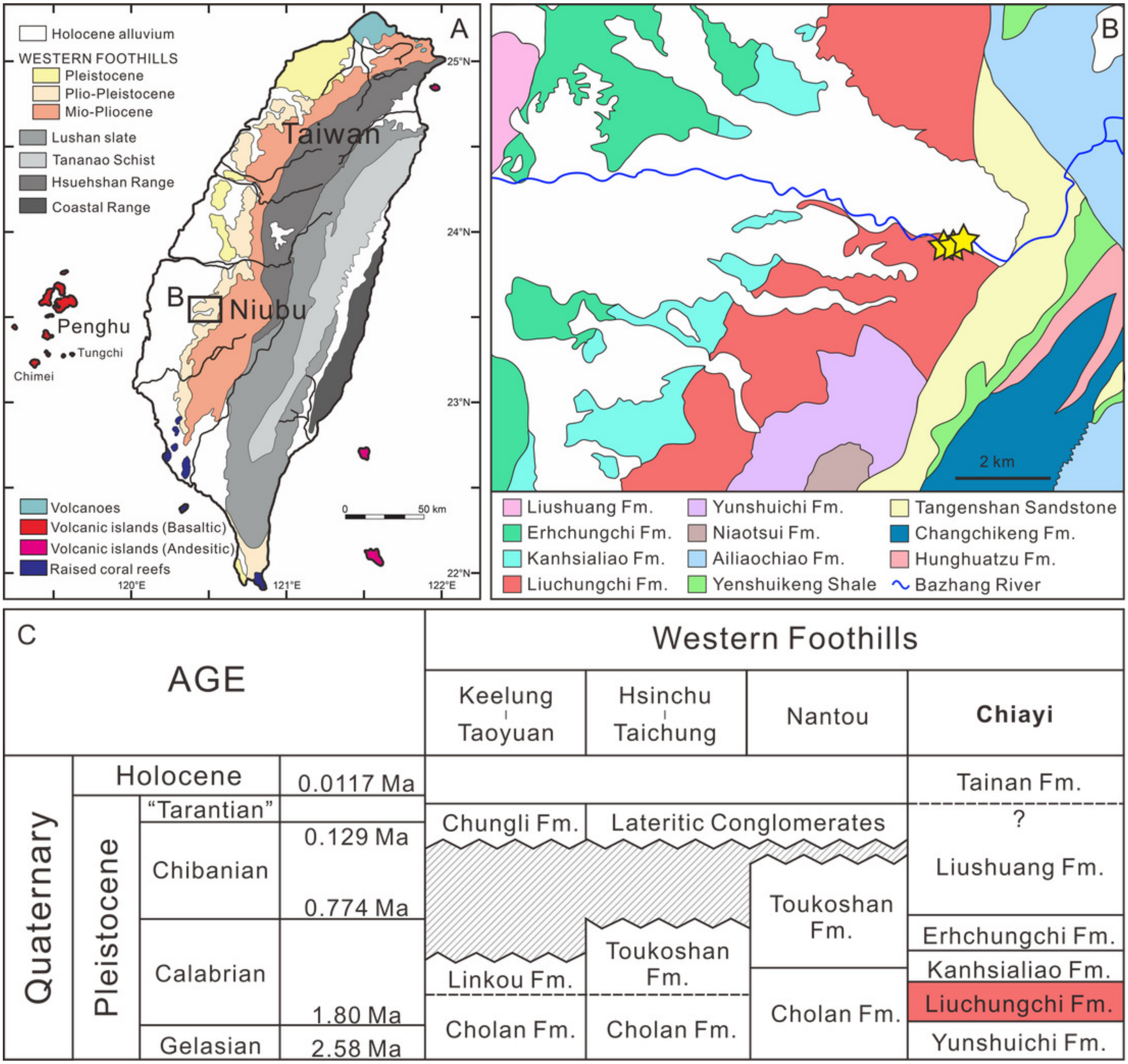
A
Holocene alluvium
WESTERN FOOTHILLS
Pleistocene
Plio-Pleistocene
Mio-Pliocene
Lushan slate
Tananao Schist
Hsuehshan Range
Coastal Range
Taiwan
B
Niubu
Penghu
Tungchi
Chimei
25°N
24°N
23°N
22°N
120°E
121°E
122°E
0
50 km
Volcanoes
Volcanic islands (Basaltic)
Volcanic islands (Andesitic)
Raised coral reefs
B
2 km
Liushuang Fm.
Erhchungchi Fm.
Kanhsialiao Fm.
Liuchungchi Fm.
Yunshuichi Fm.
Niaotsui Fm.
Ailiaochiao Fm.
Yenshuikeng Shale
Tangenshan Sandstone
Changchikeng Fm.
Hunghuatzu Fm.
Bazhang River
C
AGE
Western Foothills
Keelung - Taoyuan
Hsinchu - Taichung
Nantou
Chiayi
Quaternary
Holocene
0.0117 Ma
Pleistocene
"Tarantian"
0.129 Ma
Chibanian
0.774 Ma
Calabrian
1.80 Ma
Gelasian
2.58 Ma
Tainan Fm.
?
Chungli Fm.
Lateritic Conglomerates
Liushuang Fm.
Toukoshan Fm.
Toukoshan Fm.
Erhchungchi Fm.
Linkou Fm.
Kanhsialiao Fm.
Liuchungchi Fm.
Cholan Fm.
Cholan Fm.
Cholan Fm.
Yunshuichi Fm.

Figure 2

A, stratigraphic column (modified after Huang, 2010). B, details of the sampling sites.

GPS coordinates: Site 1 = 23°26'23.4''N, 120°35'35.5''E; Site 2 = 23°26'22.6''N, 120°35'32.7''E; Site 3 = 23°26'23.5''N, 120°35'29.8''E.

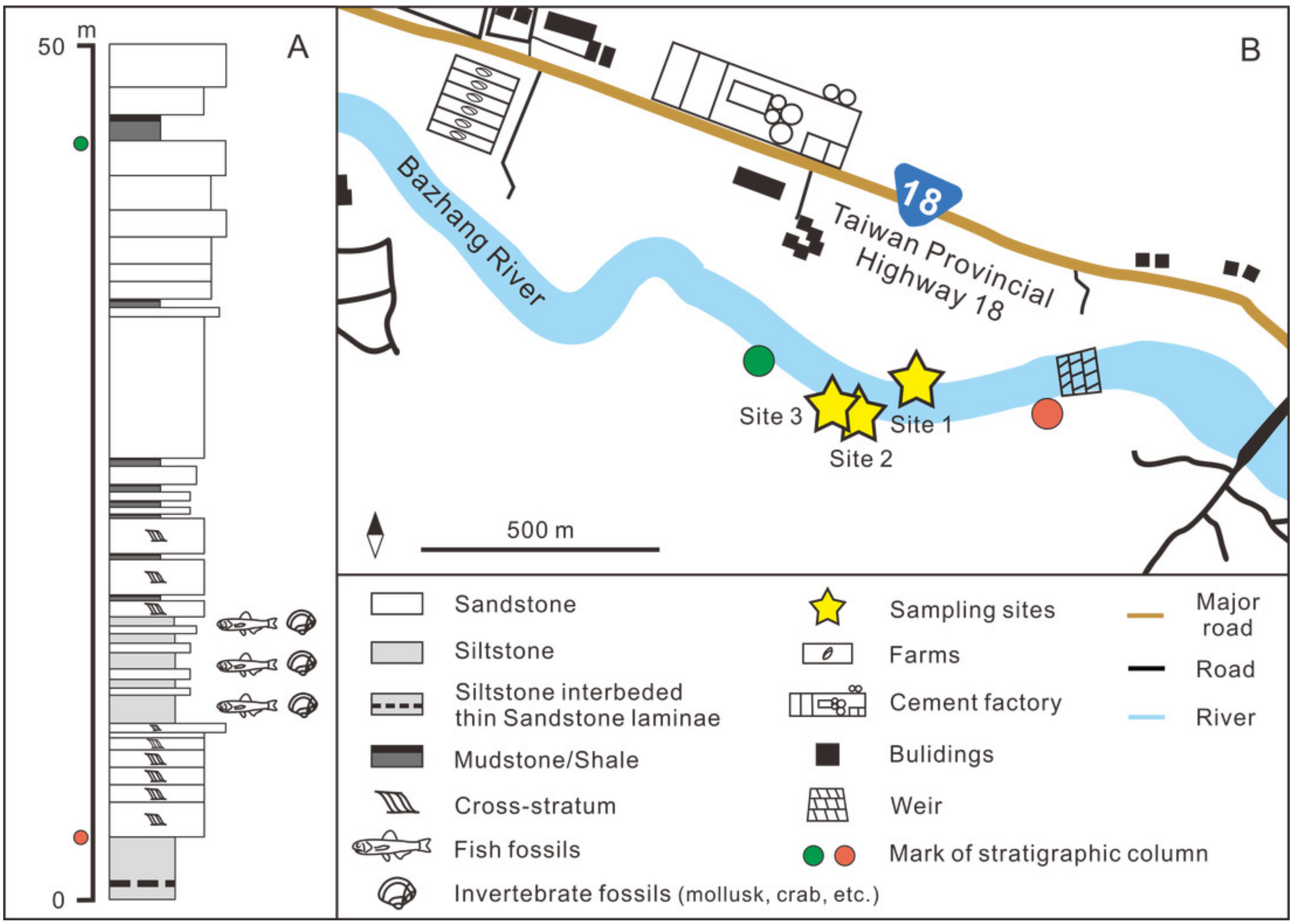

Figure 3

Shark teeth from the early Pleistocene of Liuchungchi Formation of Niubu, southern Taiwan.

A, B, *Carcharias taurus*; A, ASIZF0100320; B, CMM F0204. C, *Alopias vulpinus*, ASIZF0100532. Scale bars = 1 cm. 1 = lingual view; 2 = labial view; 3 = lateral view.

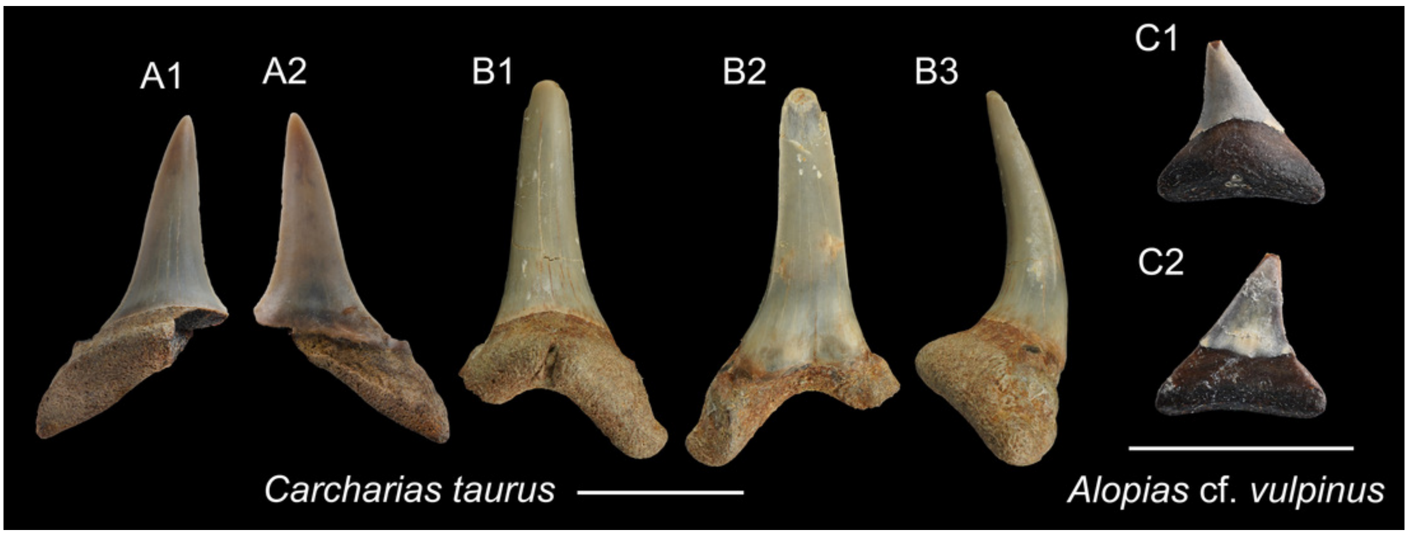

Figure 4

Carcharodon carcharias teeth from the early Pleistocene of Liuchungchi Formation of Niubu, southern Taiwan.

A, ASIZF0100344; B, ASIZF0100337; C, ASIZF0100338; D, ASIZF0100336; E, ASIZF0100335; F, ASIZF0100339; G, ASIZF0100340; H, ASIZF0100324; I, ASIZF0100328; J, ASIZF0100325; K, ASIZF0100326; L, ASIZF0100323. Scale bar = 1 cm. 1 = lingual view; 2 = labial view.

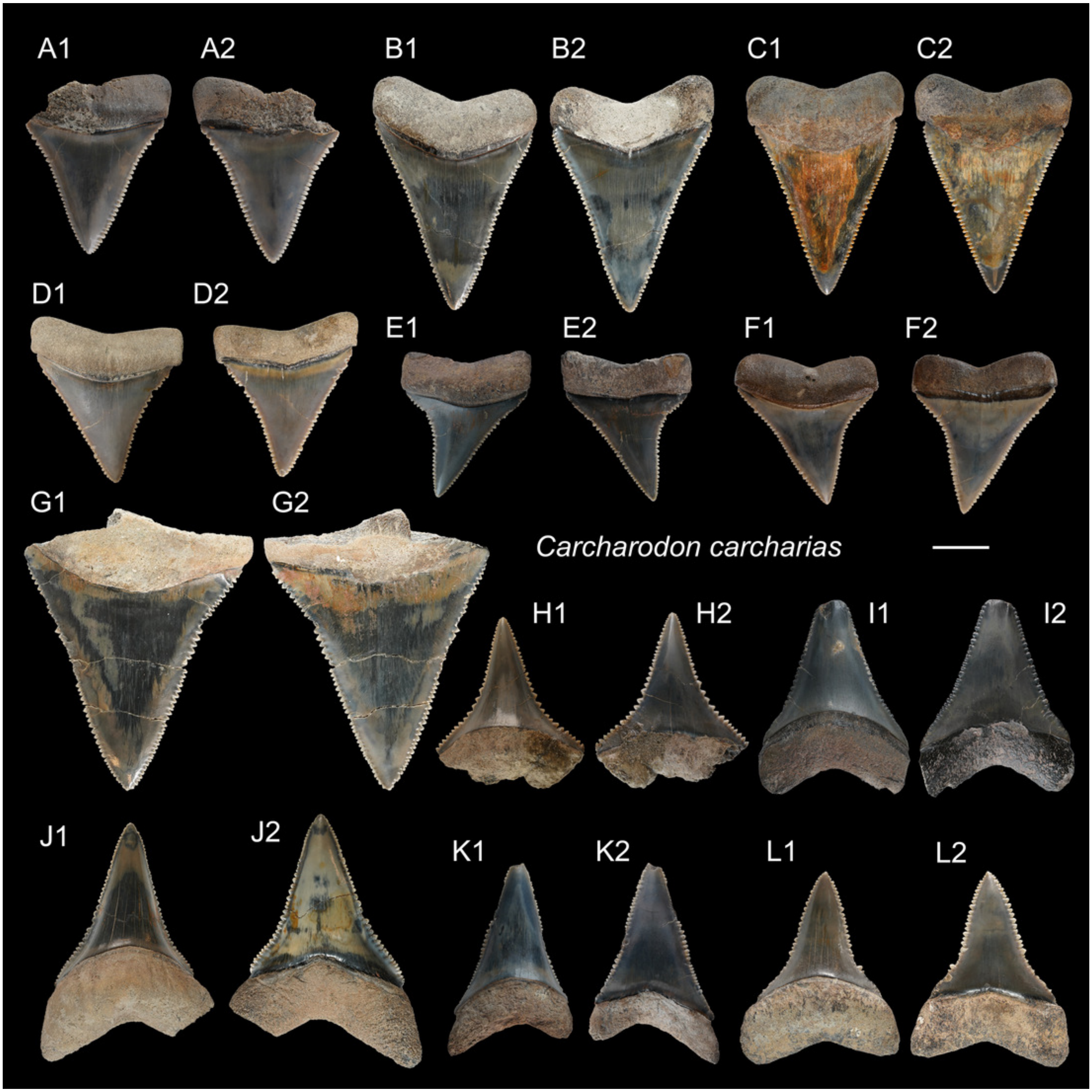
A1
A2
B1
B2
C1
C2
D1
D2
E1
E2
F1
F2
G1
G2
Carcharodon carcharias
H1
H2
I1
I2
J1
J2
K1
K2
L1
L2

Figure 5

Isurus oxyrinchus teeth from the early Pleistocene of Liuchungchi Formation of Niubu, southern Taiwan.

A, ASIZF0100317; B, ASIZF0100318; C, ASIZF0100321; D, CMM F0242. Scale bar = 1 cm. 1 = lingual view; 2 = labial view; 3 = lateral view.

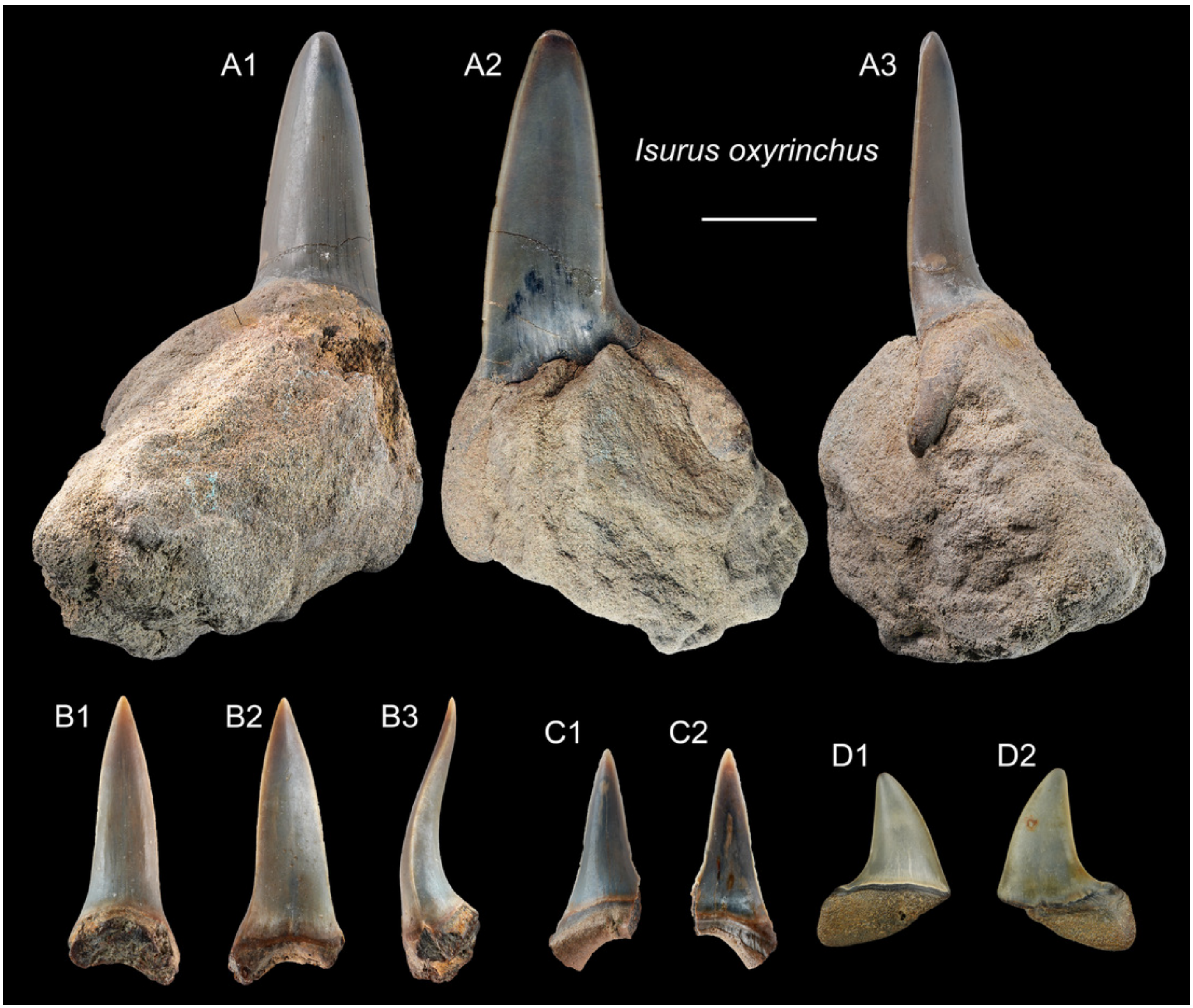

Figure 6

Shark teeth from the early Pleistocene of Liuchungchi Formation of Niubu, southern Taiwan.

A, *Hemipristis elongata*, CMM F0232. B–D, †*Hemipristis serra*; B, ASIZF0100460; C, ASIZF0100461; D, ASIZF0100462. Scale bars = 1 cm. 1 = lingual view; 2 = labial view.

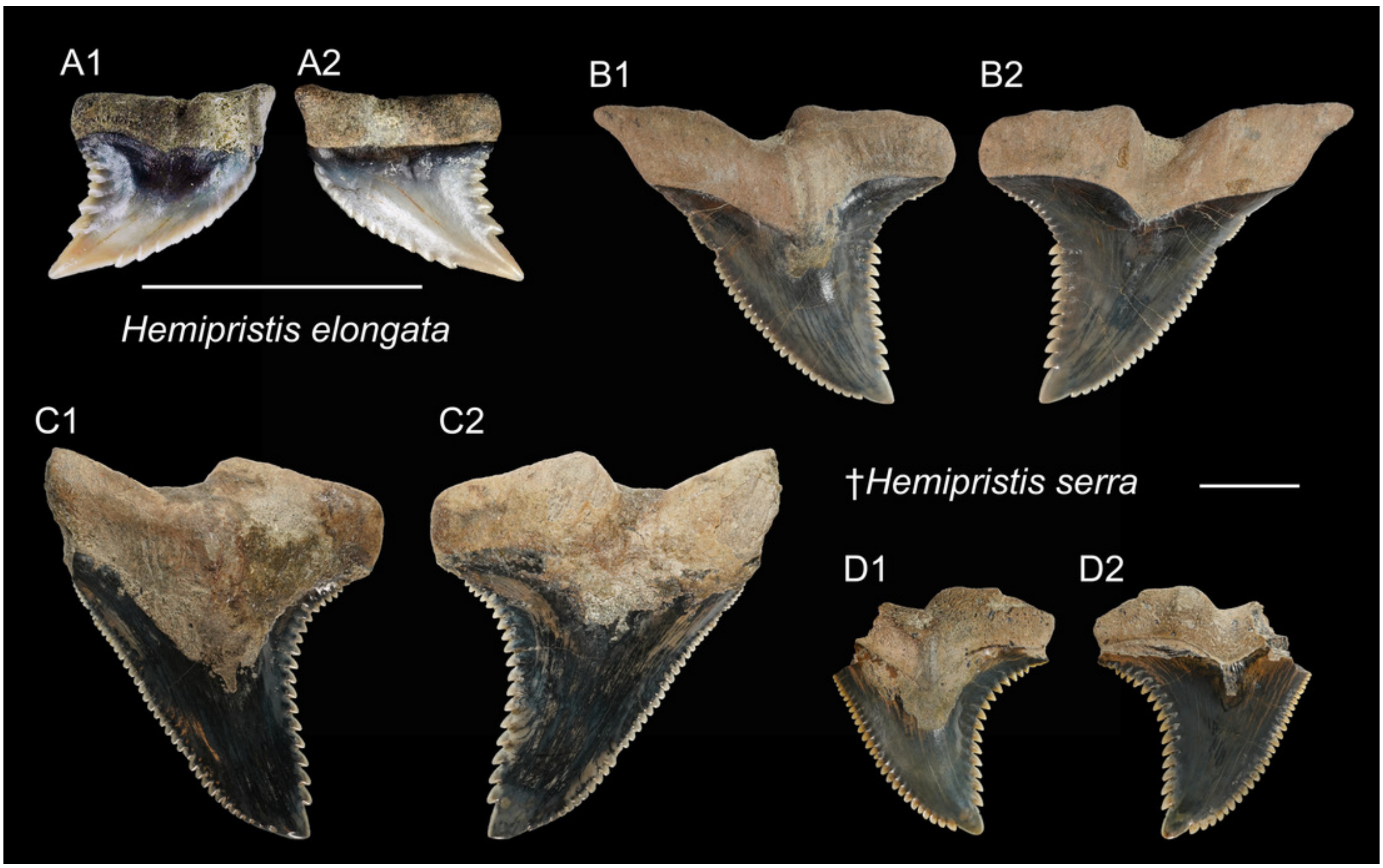

Figure 7

Carcharhinus altimus teeth from the early Pleistocene of Liuchungchi Formation of Niubu, southern Taiwan.

A, ASIZF0100357; B, ASIZF0100359; C, CMM F0363; D, CMM F0293; E, CMM F0322; F, ASIZF 0100365. Scale bar = 1 cm. 1 = lingual view; 2 = labial view.

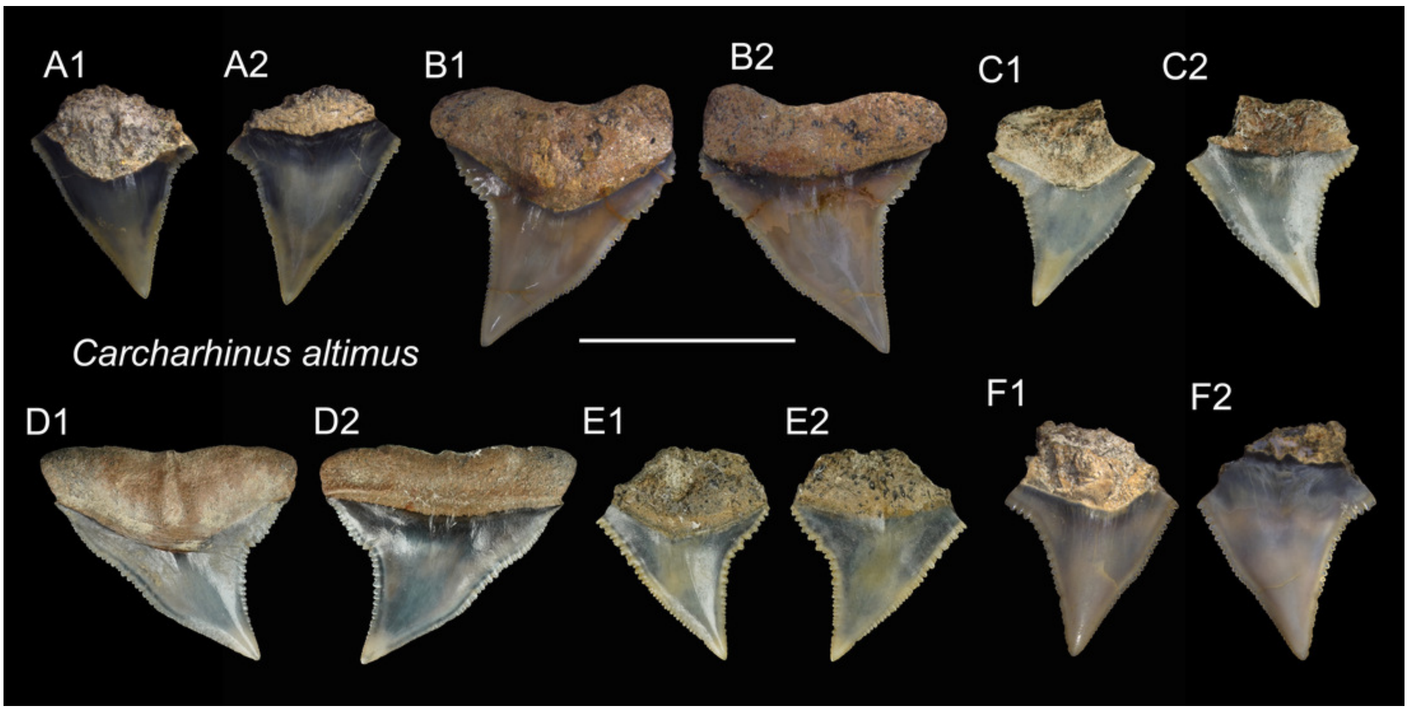

Figure 8

Carcharhinus amboinensis teeth from the early Pleistocene of Liuchungchi Formation of Niubu, southern Taiwan.

A, ASIZF 0100419; B, ASIZF0100368, C, ASIZF0100425; D, ASIZF0100366; E, CMM F0209; F, ASIZF0100369. Scale bar = 1 cm. 1 = lingual view; 2 = labial view.

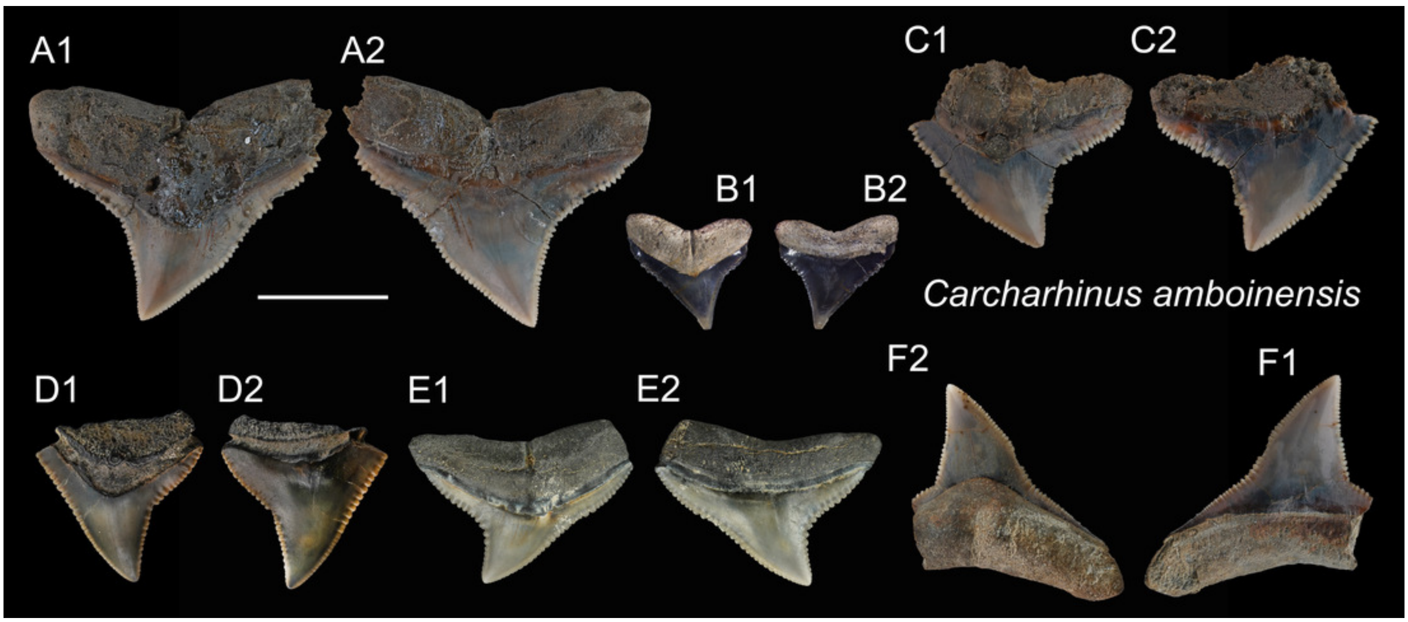

Figure 9

Carcharhinus leucas teeth from the early Pleistocene of Liuchungchi Formation of Niubu, southern Taiwan.

A, ASIZF0100398; B, ASIZF0100397; C, ASIZF0100394; D, ASIZF0100411; E, ASIZF0100396; F, ASIZF 0100395, G, ASIZF0100400; H, ASIZF0100402; I, ASIZF0100390. Scale bar = 1 cm. 1 = lingual view; 2 = labial view.

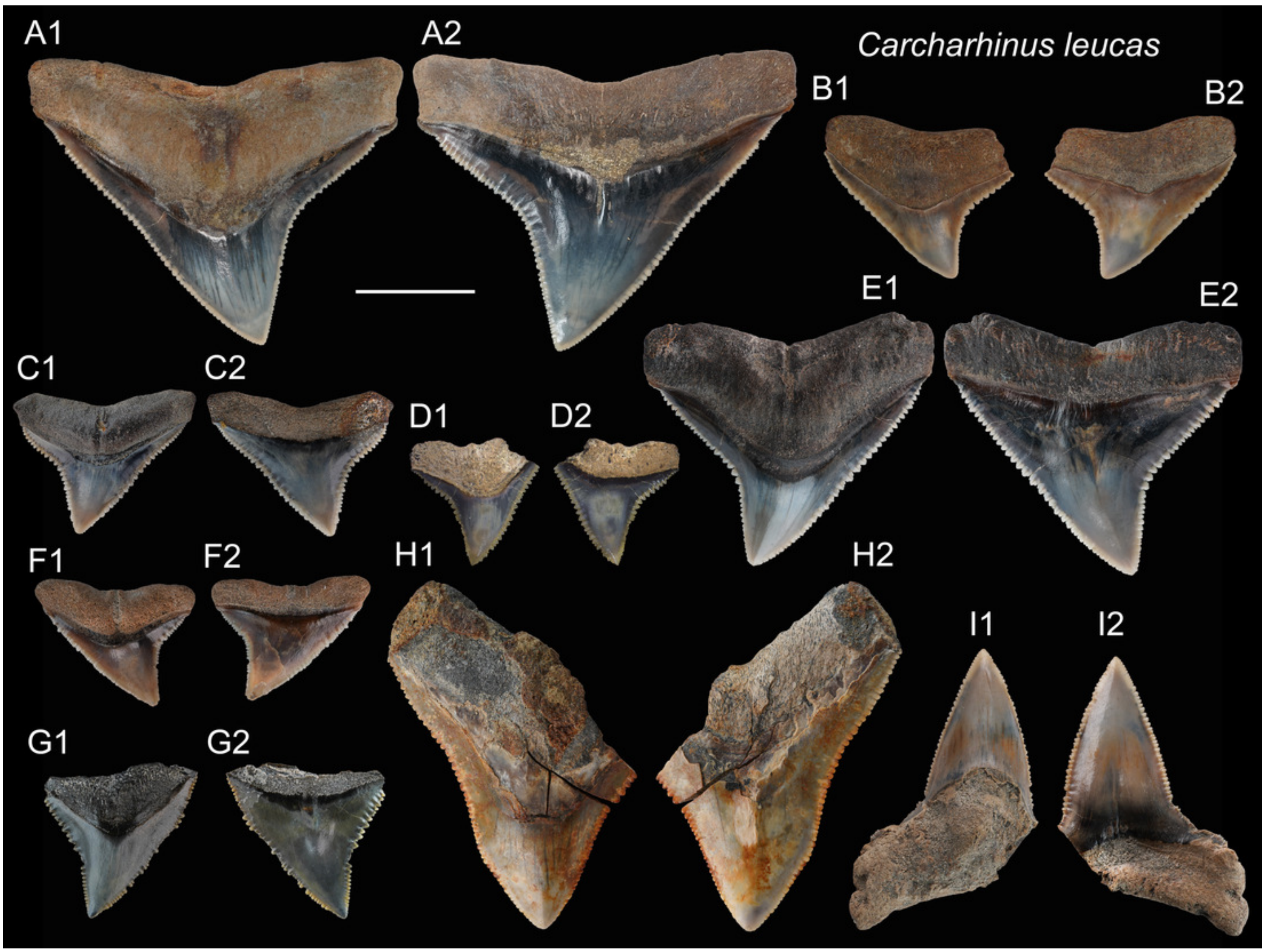

Figure 10

Carcharhinus limbatus teeth from the early Pleistocene of Liuchungchi Formation of Niubu, southern Taiwan.

A, ASIZF0100470; B, ASIZF0100476; C, ASIZF0100469; D, ASIZF0100468; E, CMM F0236; F, CMM F0111; G, CMM F0237; H, CMM F0238. Scale bar = 1 cm. 1 = lingual view; 2 = labial view.

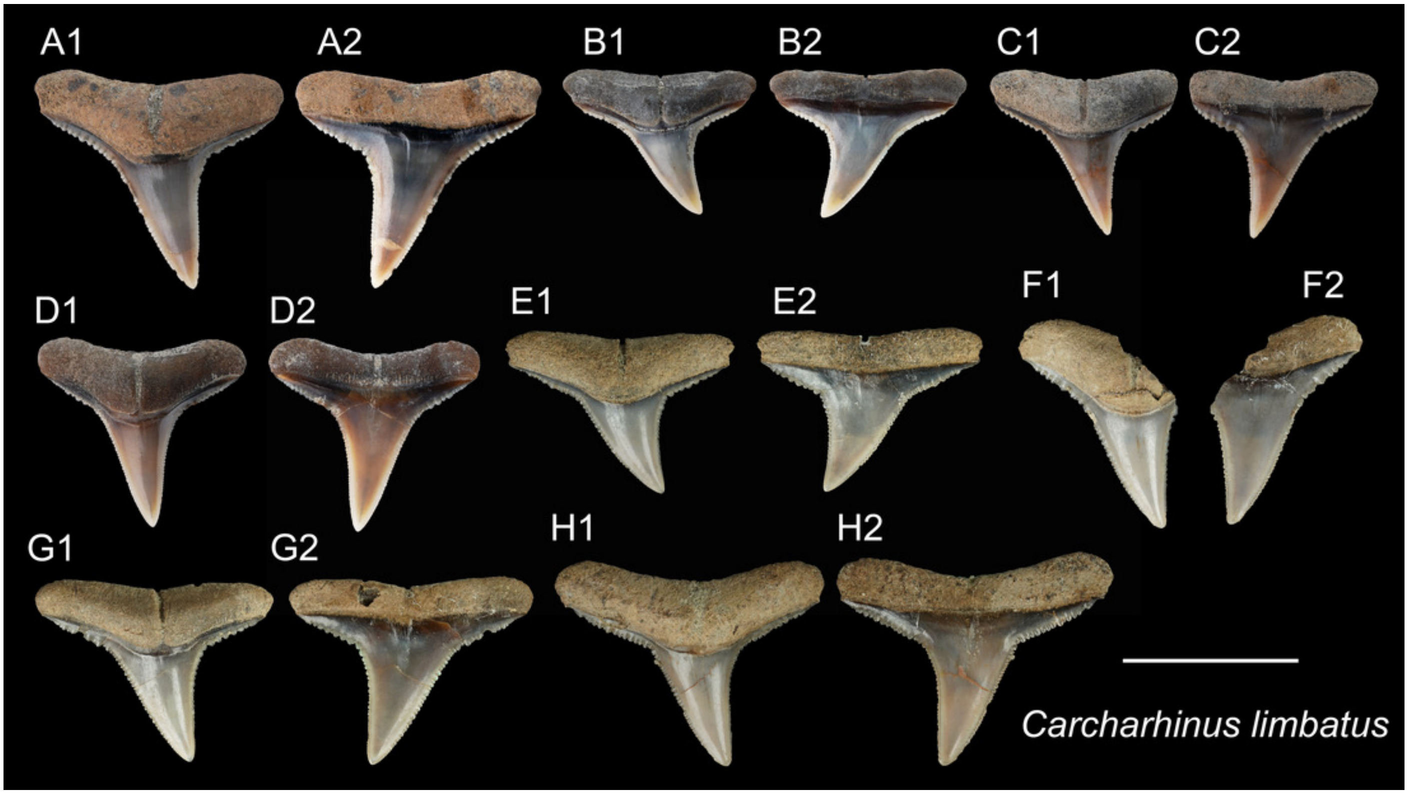

Figure 11

Carcharhinus longimanus teeth from the early Pleistocene of Liuchungchi Formation of Niubu, southern Taiwan.

A, ASIZF 0100371; B, ASIZF0100376; C, ASIZF0100370; D, ASIZF0100377; E, ASIZF0100375; F, ASIZF0100378; G, ASIZF0100374; H, ASIZF0100373; I, ASIZF0100392; J, ASIZF0100391. Scale bar = 1 cm. 1 = lingual view; 2 = labial view.

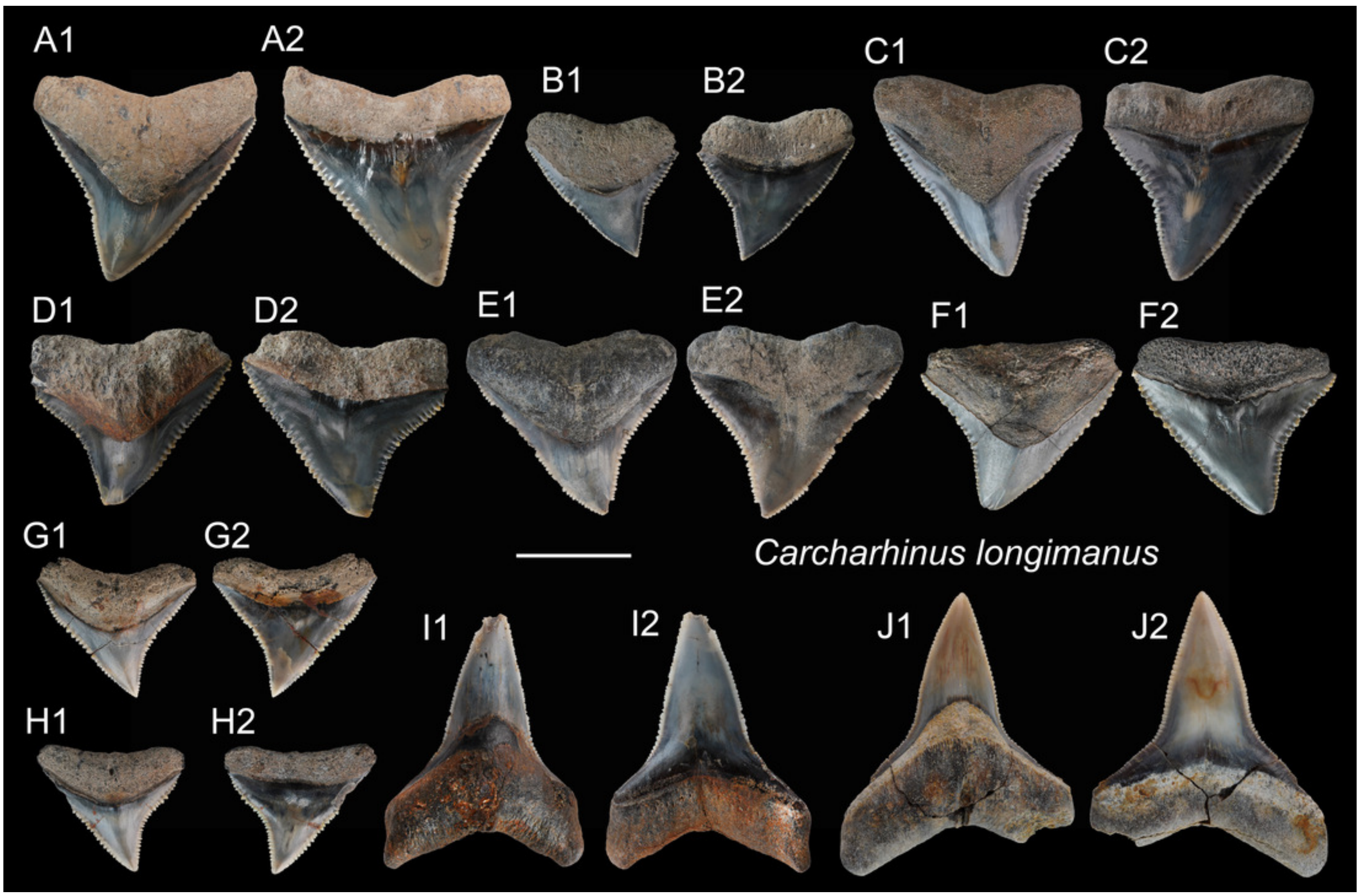

Figure 12

Carcharhinus obscurus teeth from the early Pleistocene of Liuchungchi Formation of Niubu, southern Taiwan.

A, ASIZF0100372; B, ASIZF0100384; C, ASIZF0100385; D, ASIZF0100386; E, ASIZF0100388; F, ASIZF0100387; G, ASIZF0100383. Scale bar = 1 cm. 1 = lingual view; 2 = labial view.

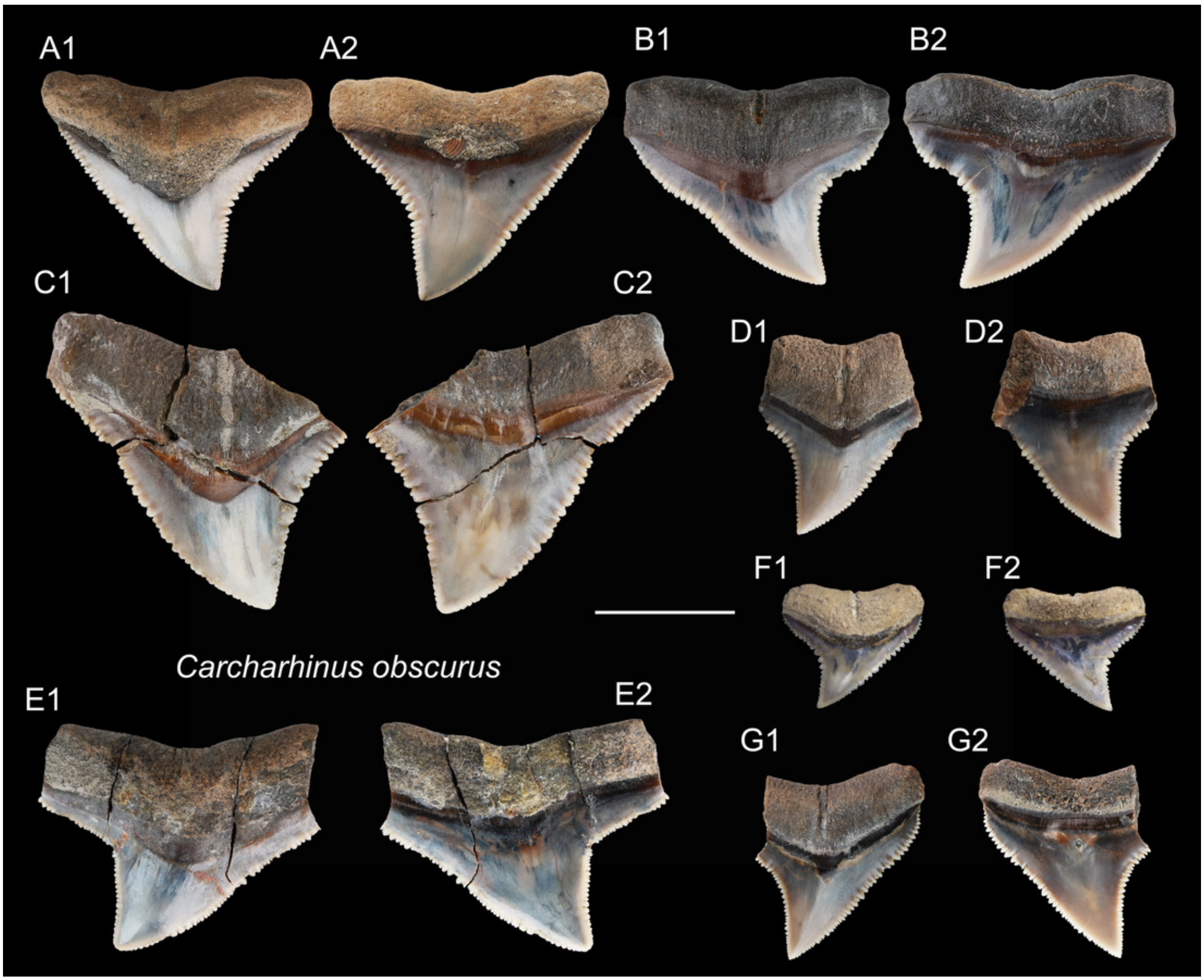

Figure 13

Carcharhinus plumbeus teeth from the early Pleistocene of Liuchungchi Formation of Niubu, southern Taiwan.

A, ASIZF0100412; B, ASIZF0100406; C, ASIZF0100405; D, ASIZF0100410; E, ASIZF0100409; F, ASIZF0100408; G, ASIZF0100407. Scale bar = 1 cm. 1 = lingual view; 2 = labial view.

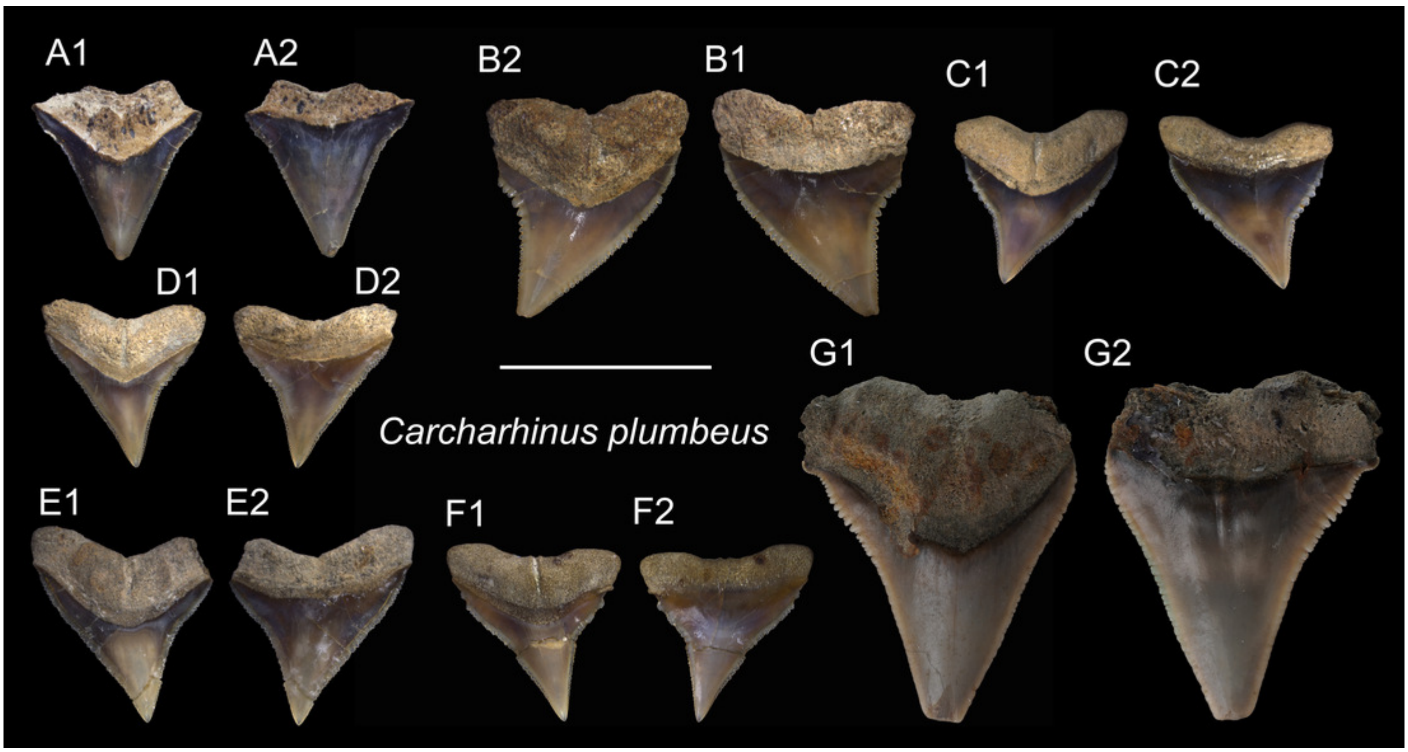

Figure 14

Carcharhinus sorrah teeth from the early Pleistocene of Liuchungchi Formation of Niubu, southern Taiwan.

A, CMM F0129; B, CMM F0119; C, ASIZF0100418; D, CMM F0126; E, CMM F0135; F, CMM F0122; G, CMM F0140. Scale bar = 1 cm. 1 = lingual view; 2 = labial view.

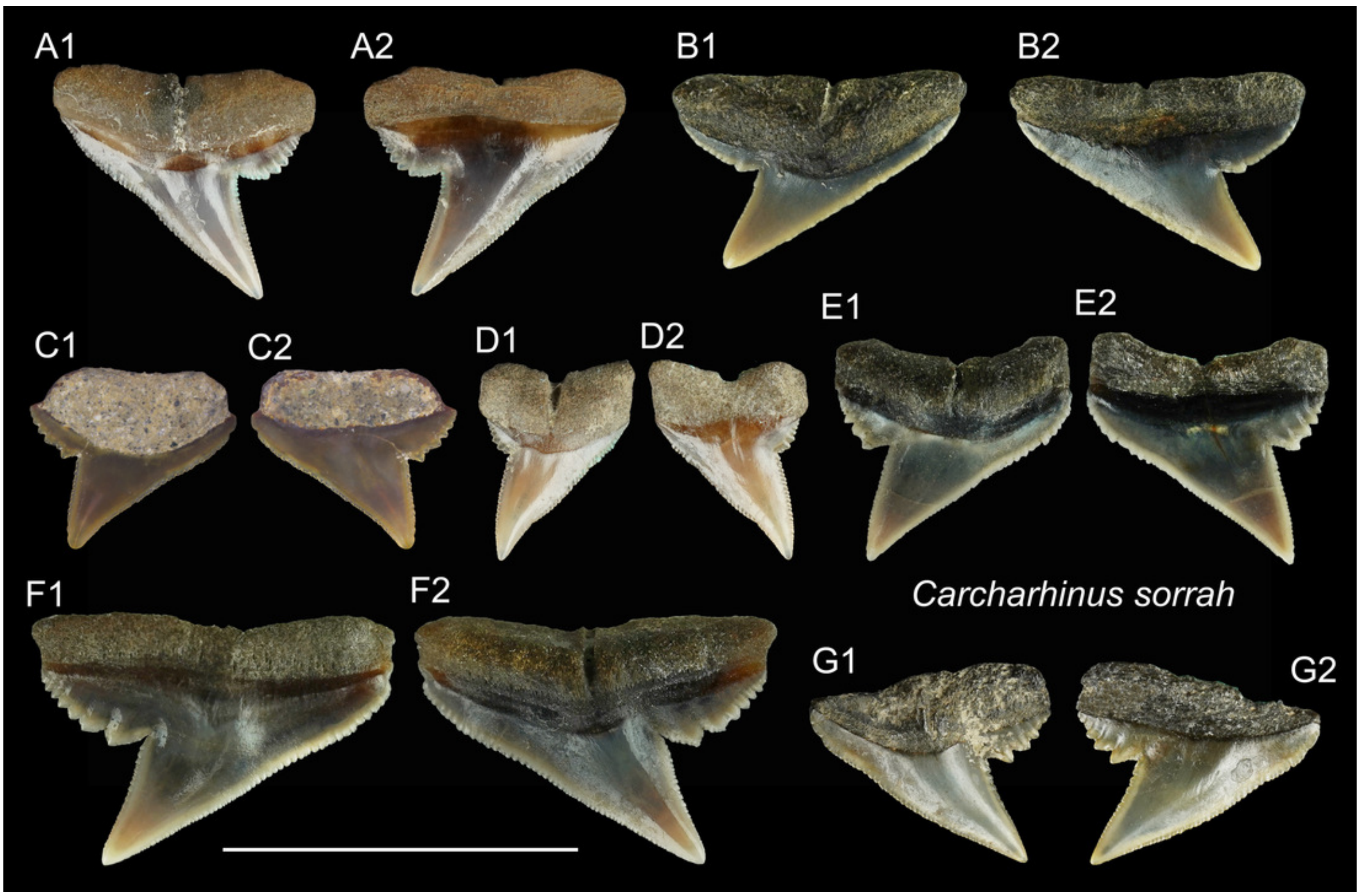

Figure 15

Carcharhinus tjutjot teeth from the early Pleistocene of Liuchungchi Formation of Niubu, southern Taiwan.

A, ASIZF0100415; B, ASIZF0100414; C, CMM F0116; D, ASIZF0100413; E, ASIZF0100417; F, ASIZF0100416; G, CMM F0323; H, CMM F0324. Scale bar = 1 cm. 1 = lingual view; 2 = labial view.

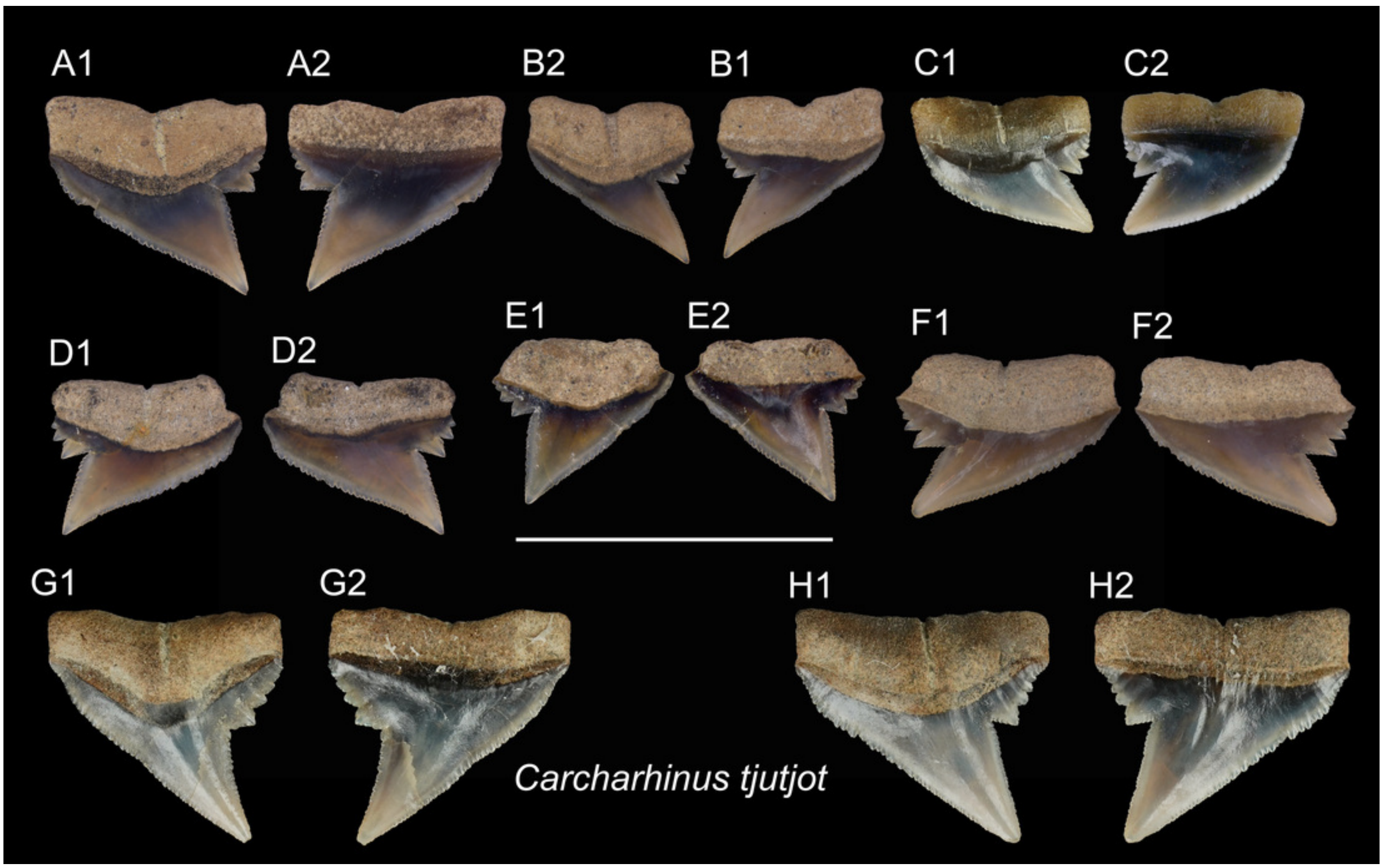

Figure 16

Shark teeth from the early Pleistocene of Liuchungchi Formation of Niubu, southern Taiwan.

A–C, *Negaprion acutidens*; A, ASIZF0100533; B, ASIZF0100531; C, CMM F0203. D–H, *Rhizoprionodon acutus*; D, ASIZF0100463; E, CMM F0120; F, CMM F0131; G, CMM F0121; H, ASIZF0100464. Scale bar = 1 cm. 1 = lingual view; 2 = labial view.

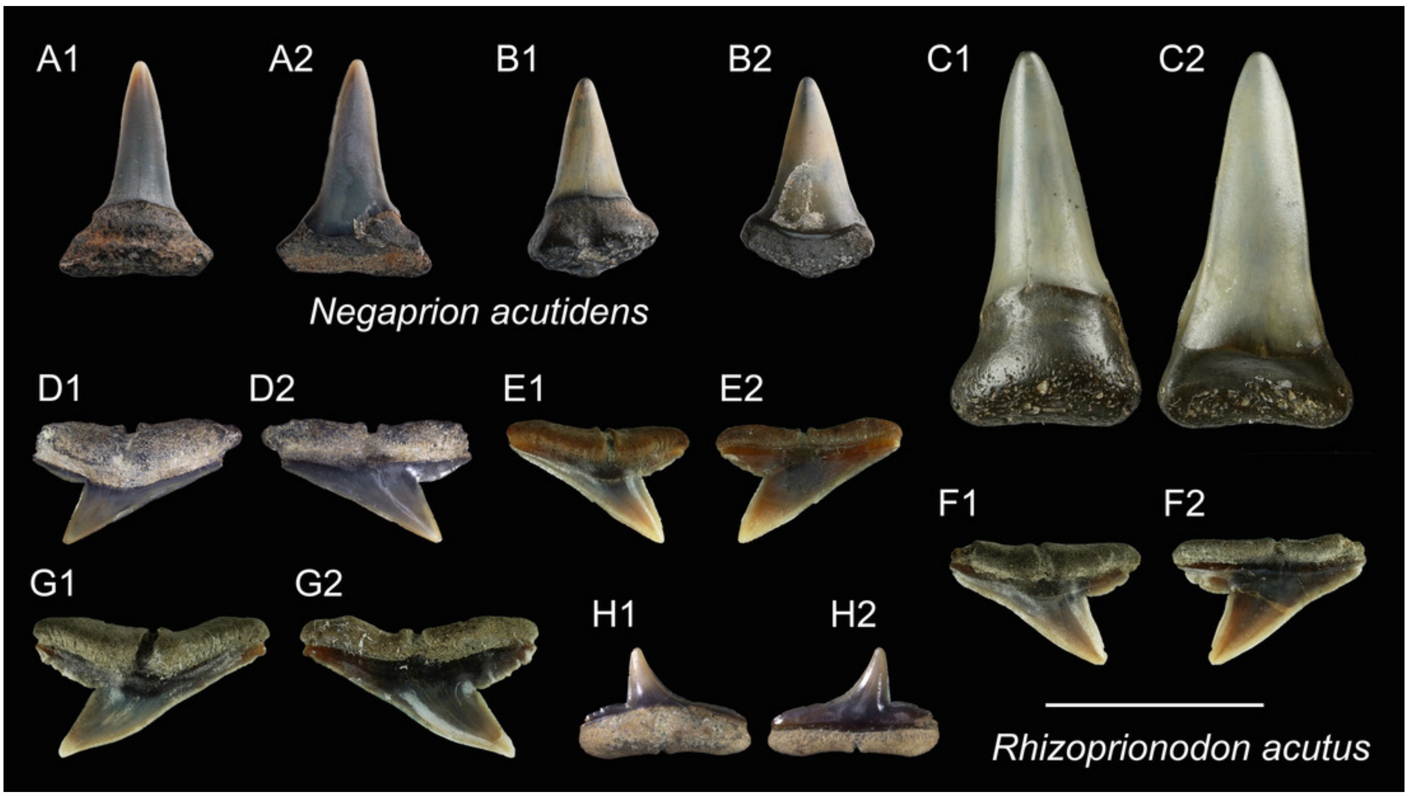

Figure 17

Shark teeth from the early Pleistocene of Liuchungchi Formation of Niubu, southern Taiwan.

A–C, *Galeocerdo cuvier*; A, CMM F0215; B, ASIZF0100459; C, CMM F0245. D, *Sphyrna lewini*, CMM F0235. Scale bars = 1 cm. 1 = lingual view; 2 = labial view.

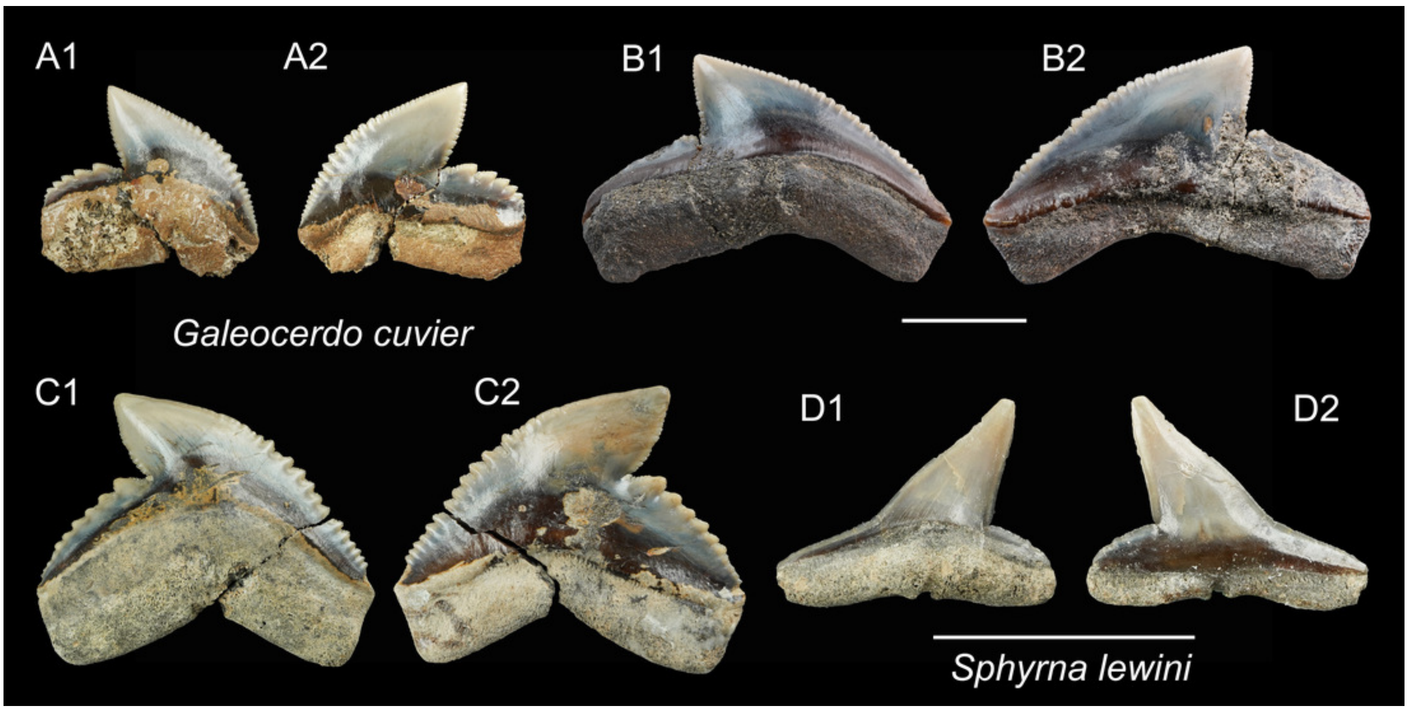

Figure 18

Dasyatis sp. teeth from the early Pleistocene of Liuchungchi Formation of Niubu, southern Taiwan.

A, ASIZF0100590; B, ASIZF0100591. Scale bar = 5 mm. 1 = occlusal view; 2 = basal view; 3 = lingual view; 4 = lateral view.

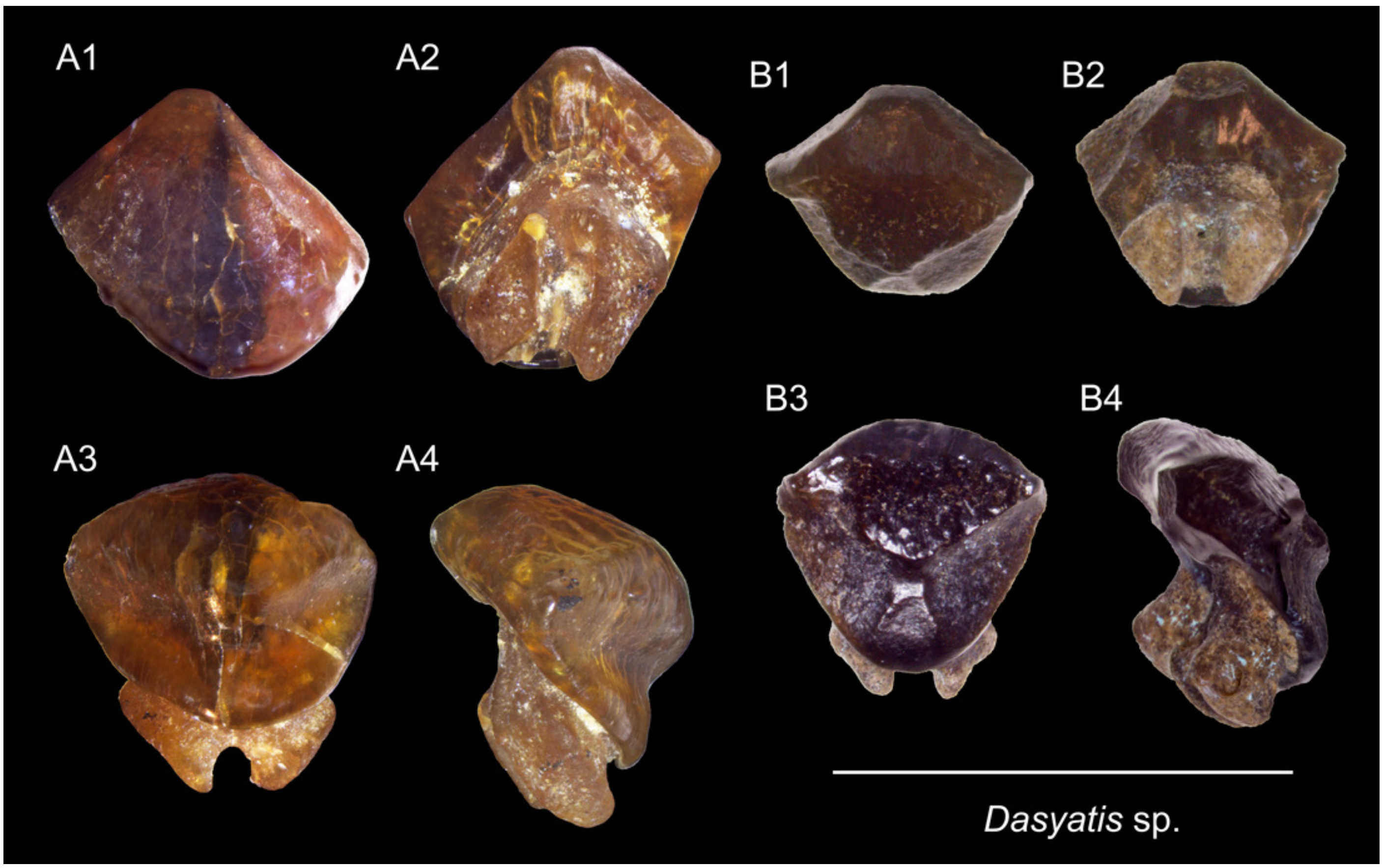

Figure 19

Aetobatus ocellatus teeth from the early Pleistocene of Liuchungchi Formation of Niubu, southern Taiwan.

A, CMM F2854; B, CMM F2850; C, CMM F0408; D, ASIZF0100549. Scale bar = 1 cm. 1 = occlusal view; 2 = basal view.

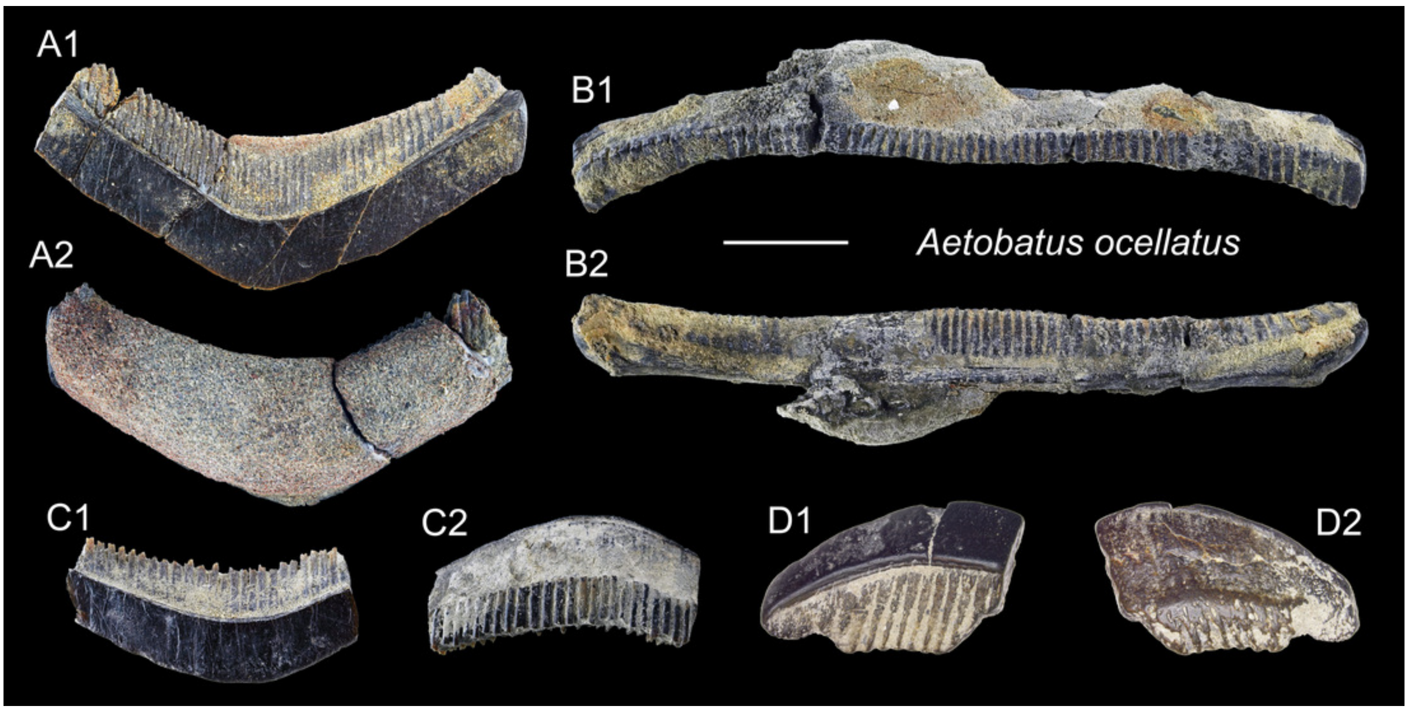

Figure 20

Myliobatis tobijei teeth from the early Pleistocene of Liuchungchi Formation of Niubu, southern Taiwan.

A, ASIZF0100582; B, ASIZF0100587; C, ASIZF0100586; D, CMM F0395; E, CMM F2855; F, CMM F0393; G, CMM F0398. Scale bars = 1 cm. 1 = occlusal view; 2 = basal view; 3 = lingual view; 4 = lateral view.

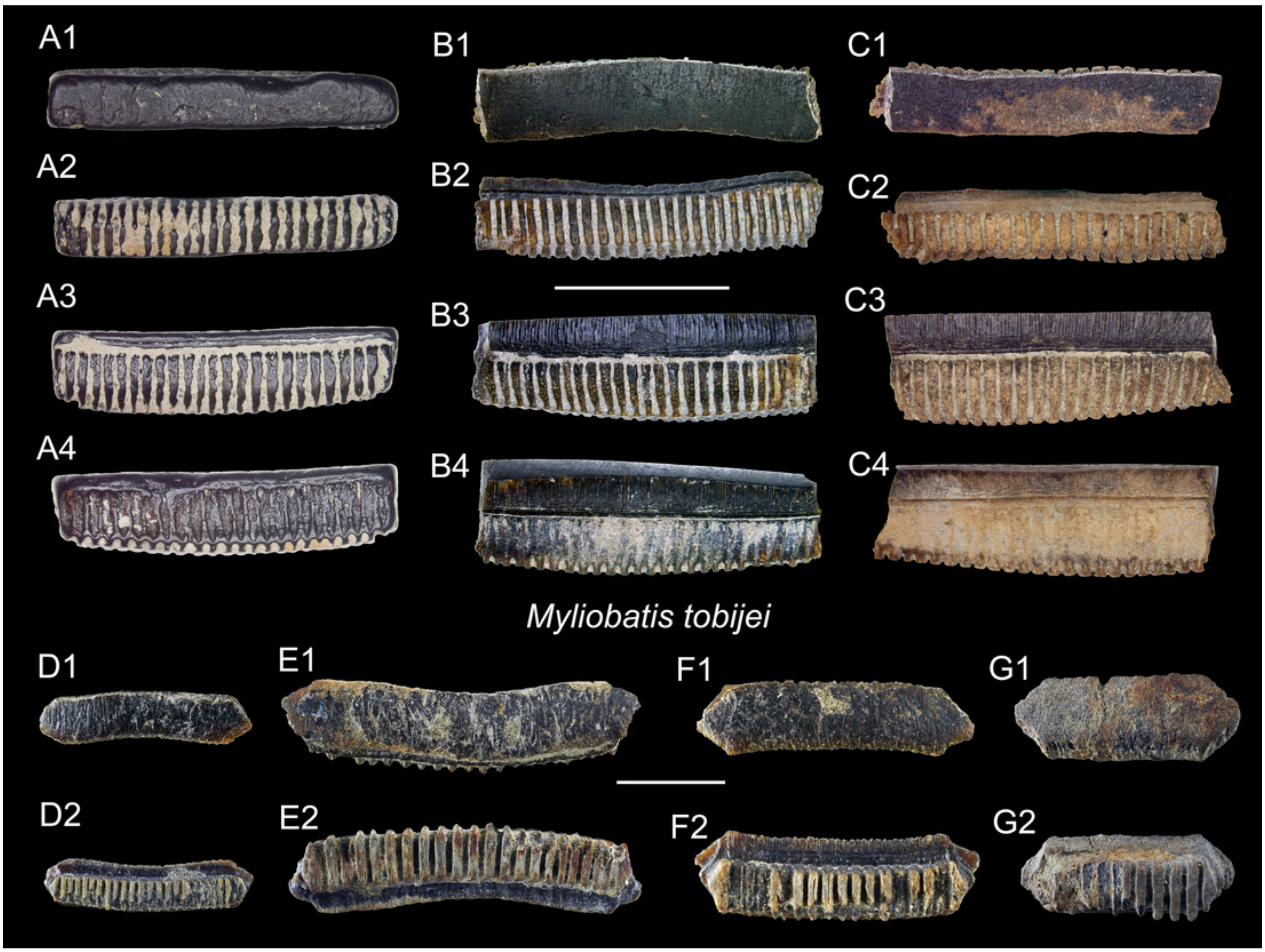

Table 1(on next page)

Elasmobranch from the early Pleistocene Liuchungchi Formation, Chiayi, southern Taiwan.

Table 1. Elasmobranch from the early Pleistocene Liuchungchi Formation, Chiayi, southern Taiwan.

Family	Taxa	ASIZF	CMM	NTM	Total
Carchariidae	*Carcharias taurus*	1	1		2
Alopiidae	*Alopias* cf. *vulpinus*	1			1
Lamnidae	*Carcharodon carcharias*	28	25	2	55
Lamnidae	*Isurus oxyrinchus*	4	1	1	6
Hemigaleidae	*Hemipristis elongata*		1		1
Hemigaleidae	†*Hemipristis serra*	3	2	1	6
Carcharhinidae	*Carcharhinus altimus*	5	10	2	17
Carcharhinidae	*Carcharhinus amboinensis*	5	2		7
Carcharhinidae	*Carcharhinus leucas*	15	53	1	69
Carcharhinidae	*Carcharhinus limbatus*	16	23	3	42
Carcharhinidae	*Carcharhinus longimanus*	18	17	2	37
Carcharhinidae	*Carcharhinus obscurus*	9	15	1	25
Carcharhinidae	*Carcharhinus plumbeus*	8	41	1	50
Carcharhinidae	*Carcharhinus sorrah*	1	10		11
Carcharhinidae	*Carcharhinus tjutjot*	5	14		19
Carcharhinidae	*Carcharhinus* spp.	88	109	10	207
Carcharhinidae	*Negaprion acutidens*	2	1		3
Carcharhinidae	*Rhizoprionodon acutus*	2	6		8
Galeocerdonidae	*Galeocerdo cuvier*	1	5	1	7
Sphyrnidae	*Sphyrna lewini*		2		2
Dasyatidae	*Dasyatis* sp.	2			2
Aetobatidae	*Aetobatus ocellatus*	32	22	4	58
Myliobatidae	*Myliobatis tobijei*	9	20	1	30
Indet.	Indet.	22	10		32
Total		277	390	30	697